

www.impactmin.eu

IMPACT MONITORING
OF MINERAL RESOURCES
EXPLOITATION

CONTRACT N°
2 4 4 1 6 6



Funded by:
European Commission
Framework Programme 7

Cooperation

Thematic Area
Environment 6.4
Earth Observation and assessment tools for sustainable development

WP7 – DEMO-SITE IMPLEMENTATION

DELIVERABLE D.7.1 REPORT ON THE KRISTINEBERG CASE STUDY INVESTIGATIONS

Compiled by
Eva Husson - LTU, Lulea University of Technology, Sweden
Fredrik Lindgren - LTU, Lulea University of Technology, Sweden
Frauke Ecke - LTU, Lulea University of Technology, Sweden

Submitted by:
GEONARDO Environmental Technologies Ltd.
(Project Coordinator)

Project Coordinator name:
Mr. Peter Gyuris

Project Coordinator organization name:
GEONARDO, Hungary

This report has been submitted to the European Commission for evaluation and for approval. Currently the content of this report does not reflect the official opinion of the European Union. Responsibility for the information and views expressed in the report therein lies entirely with the author(s).

Table of contents

LIST OF FIGURES	3
FIGURE 2-1. SITE MAP OF THE KRISTINEBERG MINING AREA.	3
FIGURE 3-1. GEOGRAPHIC LOCATION OF THE STUDY AREA.	3
FIGURE 3-2-1. UNMANNED AIRCRAFT SYSTEM (UAS).	3
LIST OF TABLES	3
1 SUMMARY.....	4
2 BACKGROUND.....	5
2.1 The Kristineberg area	5
2.2 Riparian vegetation and environmental assessment	7
2.3 Remote sensing of vegetation and biomass	7
2.4 Aim of study.....	7
3 MATERIAL AND METHODS.....	9
3.1 Study area.....	9
3.2 Aerial survey	10
3.3 Field survey, sampling and data acquisition.....	10
3.4 Vegetation mapping	13
3.5 Biomass estimation.....	13
3.6 Metal storage in vegetation	14
3.7 Assessment of biodiversity.....	15
3.8 Statistical analysis	16
4 RESULTS	17
4.1 Water chemistry	17
4.2 Vegetation chemistry.....	18
4.3 Area of vegetation classes and vegetation biomass.....	21
4.4 Metal storage in and biomass of dominating riparian species.....	22
4.5 Biodiversity	23
5 DISCUSSION	24
6 ACKNOWLEDGEMENTS.....	26
7 REFERENCES	27
8 APPENDIX I.....	31

List of figures

Figure 2-1. Site map of the Kristineberg mining area.

Figure 3-1. Geographic location of the study area.

Figure 3-2-1. Unmanned aircraft system (UAS).

Figure 3-2-2. Measurement of control points and example of biomass sampling.

Figure 3-2-3. Core zone at L3.

Figure 3-4. Vegetation map of non-submerged vegetation.

Figure 4-1. Cd, Cu and Zn concentrations \pm *SD* in Vormbäcken

Figure 4-2-1. Mean plot + *SD* of Cu concentrations in riparian vegetation in belt I-V

Figure 4-2-2. Mean plots + *SD* of Cd concentrations in riparian vegetation at L1 – L3

Figure 4-2-3. Mean plots + *SD* of Cu concentrations in riparian vegetation at L1 – L3

Figure 4-2-4. Mean plots + *SD* of Zn concentrations in riparian vegetation at L1 – L3

Figure 4-2-5. Multidimensional Scaling diagram.

Figure 4-5. Biodiversity along the three localities at Vormbacken.

List of tables

Table 3-1. Summary of dominating riparian species and species from the river channel that were sampled for chemical analyses.

Table 4-1. Amount [kg] of Cd, Cu, and Zn transported by Vormbäcken during the growing season in 2011 at L1 – L3.

Table 4-3. Area (A) and biomass (Bm) of core zone and extension zones I and II at Locality L1, L2, and L3.

Table 4-4-1 Biomass (Bm) and amount of stored Cd, Cu and Zn in dominating riparian species.

Table 4-4-2. Proportion [%] of Cd, Cu and Zn stored in riparian vegetation at L1 – L3 compared to the total amount transported by the water of Vormbäcken during the growing season.

Appendix 1. Identified vegetation classes

1 SUMMARY

The Kristineberg area is heavily impacted by mining and has a so far only roughly known environmental legacy. One river, Vormbäcken drains greater parts of the mining site at Kristineberg. The river is characterized by a riparian zone, i.e. the transition zone between water and land, of varying width. Riparian zones have important ecological and regulatory functions in aquatic systems. Quantifying plant biomass and to it related processes such as element allocation has so far been a major challenge at the scale of entire riparian zones. Here, we applied high resolution (5 cm) remote sensing with an unmanned aircraft system (UAS) in combination with field sampling. We quantified diversity and biomass of riparian vegetation at three localities (river stretches of 320 m length) along the mining-impacted river Vormbäcken and estimated the amount of metals (Cd, Cu, and Zn) stored in the dominating species.

A vegetation map at the species-level was derived from aerial images acquired with the UAS in combination with field sampling of species composition and cover. Assessments of biomass (herbaceous and shrub vegetation) and metal contents were derived by combining the vegetation maps with results from field sampling. Concentrations of Cd, Cu and Zn decreased with increased distance from Hornträsket in Vormbäcken. According to the standards of the Swedish Environmental Protection Agency, Cd and Cu concentrations ranged from high to moderate and Zn concentrations ranged from very high to moderate. Productivity of the riparian zone decreased with increased distance from the source of contamination from 9.4 to 5.4 t/ha. For metals, the total amount of vegetation-bound Cd and Zn decreased from 988 to 9 and from 136240 to 4385 g, respectively. Biomass and metal contents showed large variation between species. *Salix* sp. comprised only 15% of the total biomass of dominating species but contained 94% of all Cd and 62% of all Zn. In contrast, *Carex rostrata/vesicaria* comprised 75% of the total biomass of dominating species and contained 75% of all Cu. Biodiversity and species composition of vegetation appeared to be unaffected by potential contaminants in Vormbäcken.

Our study supports previous studies showing that the closed mines upstream of the Kristineberg mine are the main cause of the high concentrations of metals in Vormbäcken. Further, our study demonstrates the applicability of UAS for monitoring entire riparian zones. The method offers high potential for accurate assessment and modelling of nutrient and trace element cycling in the riparian zone and for planning potential phytoremediation measures in polluted areas.

2 BACKGROUND

2.1 *The Kristineberg area*

Kristineberg is located approximately 175 km south-west of Luleå in the Lycksele municipality of Västerbotten County, northern Sweden. The Kristineberg mine is part of the Skellefte mining district, one of three major mining areas in Sweden. The population of the Kristineberg municipality is 12,506 within an area of 5636 km². The landscape is dominated by coniferous forest (mainly Scots pine and Norway spruce), forest-mire complexes, mires and waterbodies. The vegetation period is on average ca. 150 days and the length of snow cover period is 150 days. The annual mean temperature is 1-2°C (February: -7 °C, June: 12 °C). Annual mean precipitation is ca. 600 mm.

The Kristineberg mining area (~300 ha) comprises a large tailings area and five mines, a large central industrial area that includes an old concentrator and three open pits. The mine has been operating since 1918. The mill was closed in 1991 due to decreasing tonnage to the mill and increasing milling costs as a consequence of closure of a number of small mines. Today, the ore is transported to the Boliden concentrator using 50-ton highway trucks, which are also used for transportation of backfill tailings to the mine. The mill capacity was gradually expanded from the original level of 300 000 tonnes per year, up to 1 million tonnes per year, a level that prevailed during the 1970's and 1980's. Today the main products recovered from the ore are zinc, copper and lead concentrates. The five ponds in the mining area (Figure 2-1) are located along a valley between two mountain ridges. Initially, the tailings were deposited in two ponds, no 1 and 2, along the Rävliomyrbäcken creek, which was diverted to bypass the ponds. In the 1950s, these ponds were filled up, and a new pond, no 3, was constructed south of the confluence between Rävliomyrbäcken and Vormbäcken. Later, a fourth pond was constructed downstream. The ponds 3 and 4 contain most of the tonnage. A fifth pond, pond 1B, was constructed to be used as an intermediate storage pond for low grade pyrite and pyrrhotite, that was intended to be sold for sulphuric acid production. As the market for such products never developed, the material was left in the pond. At closure, the tailings area consisted of five individual ponds containing pyrite-rich tailings, including three old drained ponds containing weathered tailings (ponds 1, 1B and 2); one recently operated pond containing unweathered material (pond 4); and one pond also containing substantial quantities of precipitates from the treatment of acidic mine water (pond 3).

The bedrock consists of ca.1.9 Ga metamorphosed orebearing volcanic rocks overlain by metasedimentary rocks. The metasupracrustals display a marked foliation and extensive sericitization. Pyrite-rich massive sulphide ores are intercalated within a stratigraphic unit consisting of mainly basic volcanic and redeposited volcano-clastic rocks.

Common ore minerals are pyrite (FeS₂), chalcopyrite (CuFeS₂), sphalerite (ZnS), galena (PbS) and magnetite (Fe₃O₄). Common gangue minerals include quartz (SiO₂), sericite (KAl₂(AlSi₃)O₁₀(OH)₂), chlorite (Fe,Mg,Al)₄₋₆(Si,Al)₄O₁₀(OH)₈, talc (Mg₃Si₄O₁₀(OH)₂), biotite (K(Mg,Fe)₃(AlSi₃)O₁₀(OH)₂), and calcite (CaCO₃) (Holmström et al., 2001).

The dominating soil type in the area is till with incidence of gravel, sand, peat or none or thin cover of quaternary deposits.

Waterborne pollutants and their impact on the environment (abiotic and biotic) are the main concern at Kristineberg.

The water leaving impoundment 4 enters the small river Vormbäcken. Vormbäcken starts downstream from the lake system Sörsjön-Holmträsket-Norrsjön, almost 2.5 km upstream from the outlet from the mine area at Kristineberg, and flows for approximately 40 km before joining the river Vindelälven at Vormsele. Vindelälven is a primary tributary to the river Umeälven, which in turn enters the Bothnian Sea at Umeå.

The major tributaries to Vormbäcken are drainage from the lake Holmtjärn, and the rivers Kimbäcken, Svältamyrbäcken, Svartbäcken, and Rökån. Approximately 14 km downstream from the Kristineberg mine, Vormbäcken joins Rökån. Before entering Vindelälven, Vormbäcken flows through the 8-km² lake Vormträsket. The difference in elevation between Sörsjön-Holmträsket-Norr sjön and Vormsele is about 130 m. The catchment area of Vormbäcken is approximately 370 km². In the catchment, the vegetation is dominated by coniferous forests and wetlands. The soil is moraine, and the bedrock is mainly composed of granite (Brånin et al., 1976). Mining activities have taken place at several locations in the uppermost part of the catchment area since the 1940's. The Kristineberg mine is the only mine in the area that is still active. The mines at Rävliiden, Hornträsket, and Kimheden have all been reclaimed. However, recently the Mauliden mine has been opened.

In the case of Vormbäcken, the water quality at Vormsele is to a large extent the result of mixing the original river water with the water leaving impoundment 4, surface water from the tributaries, and groundwater from the rest of the catchment area.

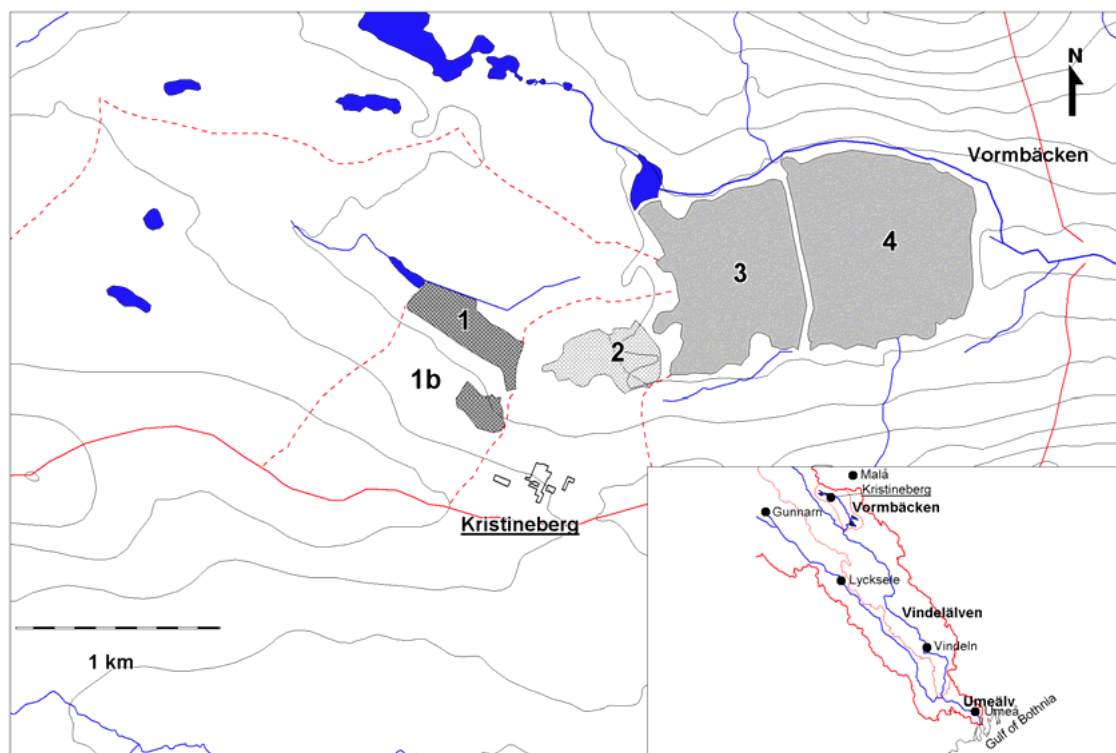


Figure 2-1. Site map of the Kristineberg mining area showing the different ponds (impoundments) and local water catchment area at Kristineberg. The dashed lines marks identified sub-catchment areas. From Höglund and Herbert (2004).

Upstream from the Kristineberg mine, the river water has a pH close to 6, and the water contains approximately 6 mg DOC/l and 0.2 mg Fe/l (Sjöblom et al., 2004). A substantial part of the Fe has been found to occur in particles of 1 kDa – 0.2 µm size (Forsberg, 2002). At present, the concentrations of Cd, Cu, and Zn in the river water are elevated already upstream from the outlet from the mining area at Kristineberg (Sjöblom et al., 2001). This is probably due to a combination of earlier mining activities and the local geology (cf. Runnells et al., 1992). During normal operation of the water treatment facilities at Kristineberg, the treated water actually dilutes the river water with respect to the trace metals mentioned above (Sjöblom et al., 2001). However, the treated drainage is a

significant source of Ca to the river water. Sampling in 2000 (Sjöblom, 2003) showed that the concentration of Cd, Cu and Zn in all of the tributaries investigated was much lower than those encountered in Vormbäcken. The natural tributaries accounted for between 4 and 12% of the loadings of Zn, Cu and Cd to the system. For lead, they accounted for between 11 and 17%. Lead appears to be mobilised from the catchment area during periods of high flow. The contribution of Fe, Al, and Mn in the river at Aspliden (that is, background upstream of the discharge from Kristineberg together with the discharge) is about half the total loading (October, 2000). For arsenic, the natural tributaries account for at least twice the loadings measured at Aspliden (where discharge is completely mixed with river water). The contribution of groundwater to the total load in Vormbäcken is also thought to be high (especially for As).

2.2 Riparian vegetation and environmental assessment

The riparian zone, i.e. the transition zone between water and land, has important ecological and regulatory functions in aquatic systems: forming wildlife habitats and ecological corridors, stabilising riverbanks, shading, providing organic matter and food for aquatic and riparian biota, increasing habitat diversity, retaining sediment and nutrient as well as pollutants, and regulating water yield (Haycock et al. 1993; Kalff 2001; Mander and Shirmohammadi 2008; Salemi et al. 2012; Strayer 2010). The importance of riparian zones has also been acknowledged by the environmental legislation of the European Union. The quality element *Morphological Conditions* refers to the structure and condition of the riparian zone and is used for the classification of the ecological status of rivers according to the Water Framework Directive (EU 2000). Vegetation plays a key role for productivity, carbon cycling as well as nutrient and trace element allocation in riparian zones and water bodies (Bishop et al. 1995; Newham et al. 2011; Richardson et al. 2007; Tabacchi et al. 1998; Tabacchi et al. 2000). Phytoremediation, i.e. mitigation of environmental problems by the use of plants, in riparian zones and wetlands (natural and constructed) is increasingly used to improve water quality in recipients (Pilon-Smits 2005; Xiang and Rengel 2009). Quantifying plant biomass and to it related processes such as nutrient and trace element uptake is therefore important to enhance our knowledge on natural processes in riparian zones and to assess phytoremediation potentials. Biomass assessment is mainly based on field sampling and restricted to small areas at the scale of sampling plots (Gibson 2002; Mueller-Dombois and Ellenberg 2002). The accurate assessment of biomass at the scale of entire riparian zones has been a major challenge.

2.3 Remote sensing of vegetation and biomass

Remote sensing approaches with different biomass-related indices (e.g. Normalized Difference Vegetation Index, NDVI, Pettorelli et al. 2005) have been used to assess the biomass of e.g. wetlands (Adam et al. 2010; Mutanga et al. 2012). However, so far they did not succeed in resolving shrub and herbaceous vegetation at the species-level, which is mainly due to the spatial resolution of available remote sensing data and limitations in automated image classification. Recently developed unmanned aircraft systems (UAS) offer new state-of-the-art methods for quantifying plant abundance and biomass. UAS not only provide cost-efficient solutions, but yield remote sensing data with sub-decimetre spatial resolution and high spatial accuracy (Bryson et al. 2010; Rango et al. 2009).

2.4 Aim of study

Here, we applied a combination of UAS remote sensing (5 cm resolution) and field sampling for mapping riparian vegetation at the species-level and assessing biomass and vegetation-bound amount of metals (Cd, Cu and Zn) at the scale of entire riparian zones along the mining-impacted river Vormbäcken in northern Sweden. The aim of this study is four-fold. Firstly, we assess biodiversity of riparian vegetation along Vormbäcken. Secondly, we quantify the biomass of riparian vegetation (total and separated for dominating species) at three localities downstream the river. Thirdly, we estimate the amount of metals (Cd, Cu, and Zn) stored in the dominating species to evaluate if the concentrations of Cd, Cu and Zn in aquatic and riparian vegetation decrease along a longitudinal and lateral gradient,

i.e. with increasing distance from the source of contamination and from the river. Finally, we evaluate the added value of sub-decimetre resolution UAS orthoimages for the assessment of biomass and element accumulation in vegetation at the scale of entire riparian zones.

3 MATERIAL AND METHODS

3.1 Study area

The study was performed along the river Vormbäcken that is located in the municipalities of Lycksele, Malå, and Norsjö, Västerbotten county, northern Sweden (ca. 65°N, 18°E). The river is located in the middle boreal sub-zone (Sjörs 1999). It originates in the lake system Hornträsket (composed of Sörsjön and Norrsjön), close to the mining area at Kristineberg. 2.5 km downstream of the outlet of Hornträsket, effluents from the tailings impoundment join the river. After 45 km Vormbäcken joins the river Vindelälven at Vormsele. Vindelälven is a primary tributary to the river Umeälven and has the Gulf of Bothnia as final recipient. The catchment of Vormbäcken is approximately 350 km² and dominated by coniferous forests and wetlands. Mining activities have taken place at several locations in the uppermost part of the catchment area since the 1930's. The Kristineberg mine is the only mine in the area that is still active. The mines at Granlunda, Rävliidmyran and Hornträsket which drain into Sörsjön and Norrsjön, respectively, the mine at Kimheden which drains into the tailings impoundment, and the mine at Rävliiden which drains into the river Kalvbäcken, a tributary to Vormbäcken, have all been abandoned. All mines except the Granlunda mine have been reclaimed after closure. Since the middle of the 1990's, Hornträsket has been characterised by high concentrations of Cd, Cu, and Zn resulting in the deterioration of the lake fauna (Jacks et al. 2005; Samuelsson 2010). Leakage from the abandoned mines, from mineralised bedrocks as well as from soils due to fluctuating ground water levels and extensive forestry (logging and ditching) were discussed as main sources of the metals (Jacks et al. 2005; Samuelsson 2010). Compared to concentrations of Cd, Cu and Zn in Hornträsket, concentrations of these elements are low in the effluent from the impoundment (Sjöblom 2003). We performed the study at three localities (L1 – L3) along Vormbäcken, 7, 15 and 23 km downstream of Hornträsket, respectively (Figure 3-1). Mean pH ranged from 6.5 at L1 to 6.7 (n = 5) at L3 in July/August 2011.

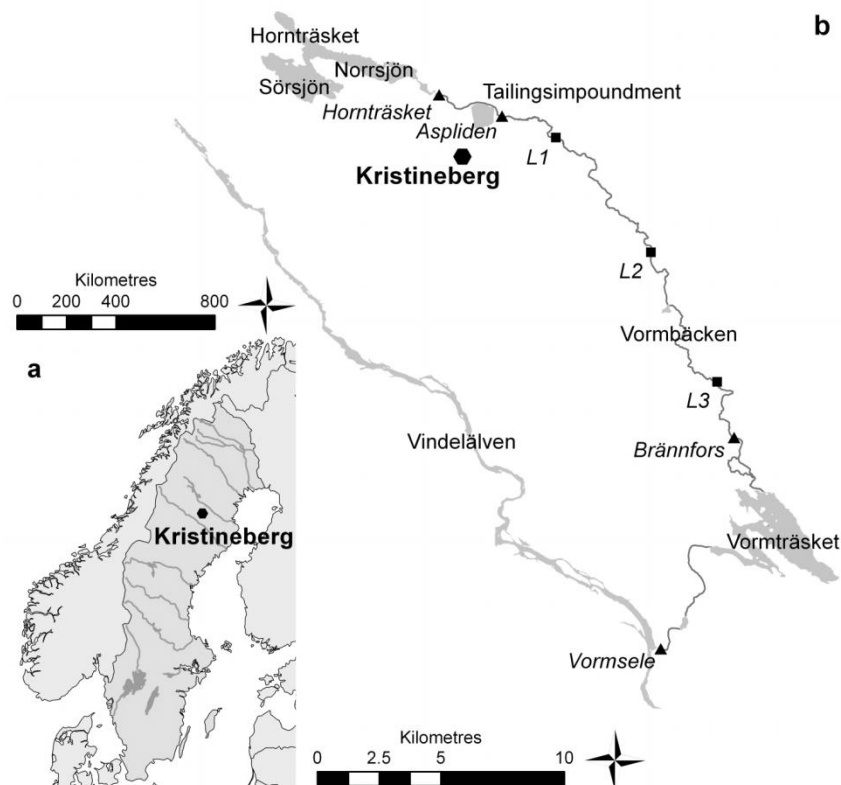


Figure 3-1. Geographic location of the study area in Sweden (a) and of the studied localities (■) and additional water sampling points along Vormbäcken (▲, b).

3.2 Aerial survey

The three localities were surveyed on 14 July 2011 with the Personal Aerial Mapping System (PAMS) developed by SmartPlanes Sweden AB (Skellefteå, Sweden). The PAMS consists of 1) an unmanned aircraft system (UAS), i.e. an ultra-light remotely controlled aircraft equipped with a digital camera with calibrated optics, autopilot and GPS (global positioning system), and a ground control station with mission planning and flight control software (Figure 3-2-1), and b) an aerial mapping software for automated on-site production of georeferenced high resolution image mosaics. For a detailed description of the system see Husson et al. (manuscript). The generated RGB (Red-Green-Blue)-images were post-processed by GerMAP GmbH (Welzheim, Germany). The resulting orthoimages had a spatial resolution of 5 cm and were georeferenced to the Swedish national grid using ground control points identified in orthophotographs from the Swedish Land Survey. For fine adjustment, we used the Georeferencing tool in ArcGIS software (ESRI 2010). Per locality, we used 15 – 20 control points to reduce the root mean square error to <10 cm. The control points were measured on site using a Carrier-Phase Enhancement Global Positioning System (CPGPS) with a spatial error of <5 cm (Figure 3-2-2).



Figure 3-2-1. Unmanned aircraft system (UAS) consisting of a remotely controlled airplane (wingspan 1.2 m) with a digital camera and a ground control station with mission planning and flight control software.

3.3 Field survey, sampling and data acquisition

Field sampling was performed at the three localities L1, L2, and L3 downstream of Horträsket and the mining area 12 July – 20 August 2011. At each locality, a 50 x 20 m area that stretched along Vormbäcken was sampled. Vegetation was sampled in five belts (I-V) parallel to the river bank that were 4 m wide. In belt I, we randomly placed 20 sample plots (50 × 50 cm) and in belt II-V 15 sample plots with a minimum distance of 2 m. In each sample plot, the cover of the five species with the highest cover was recorded according to a four-graded scale: *C1* >0 – 12%, *C2* >12 – 25%, *C3* >25 – 50%, *C4* >50 – 100%. *Salix* was treated at genus level and *Carex rostrata* and *Carex vesicaria* were combined due to the difficulties to distinguish these two species in the field. The above-ground living biomass of the five dominating, i.e. most abundant plant species, was taken from each sample plot and the total weight was recorded (Figure 3-2-2). Trees >1.5 m were not sampled. Complementary samples were taken 19 – 27 July 2012, so that we had at least three samples of biomass in each vegetation class. At L1, we sampled in total 89 plots, at L2 80 and at L3 83 plots (exemplified for L3 in Figure 3-2-3b). The number of sample plots per vegetation class ranged from 3 – 48 (mean 11). The position of all sample plots was measured with a CPGPS (Figure 3-2-2).



Figure 3-2-2. Measurement of control points and example of biomass sampling.

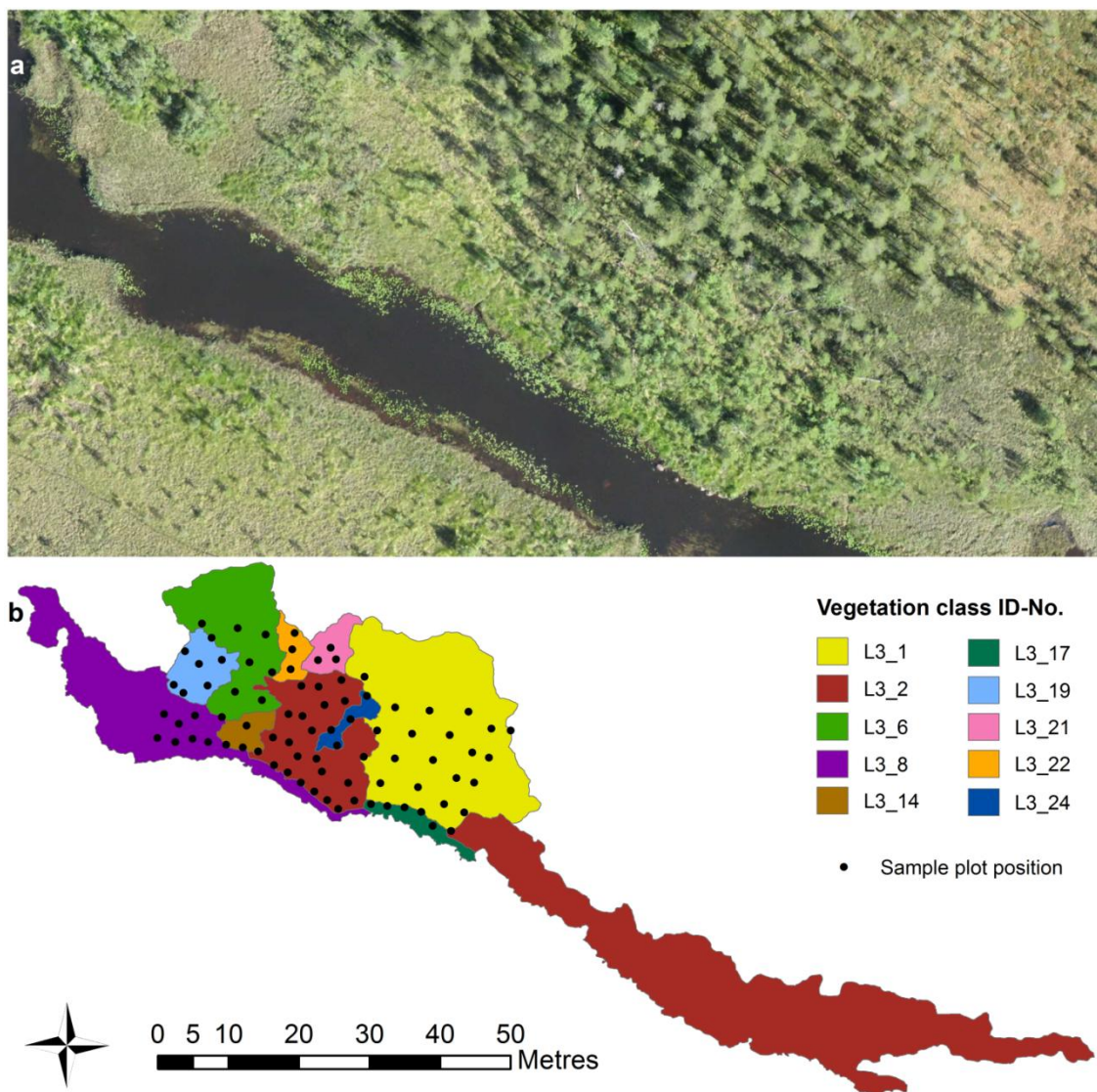


Figure 3-2-3. Core zone at L3, a) orthoimage and b) vegetation map with sample plots. For species composition of the vegetation classes see Appendix I.

For chemical analyses of riparian vegetation, we took representative samples from the two dominating plant species in each belt at each locality in July/August 2011. To get representative samples per species and belt with a minimum weight of 50 g, we collected leaves of at least 20 different specimens distributed over the whole belt by tearing or cutting with a plastic knife. At L3 belt II-V more than two species showed the same frequencies. Here, we sampled up to four species per belt. To compare one and the same species between all localities and belts, we took additional samples of the two most common species *Carex rostrata/vesicaria* and *Salix* sp. in July 2012. *Carex rostrata/vesicaria* and *Salix* sp. were also sampled at Hornträsket (one combined sample for belt I and II per species). For vegetation from the river channel, we took representative samples from the three dominating species at each locality in July/August 2011. A representative sample for the vegetation in the river channel consisted of leaves from at least 10 different specimens per species distributed along the whole 50 m long river stretch. The number of species from the river channel that were found at more than one locality in 2011 was low. To compare the same species between localities, we searched in July 2012 by boat within a stretch of 100 m up- and downstream from the sample area of each locality as well as in Hornträsket for the same species that were already sampled in July/August 2011 (see Table 3-1 for an overview of sampled species). In the afternoon of each sampling day, samples for chemical analyses were sent by mail to the ALS Scandinavia AB laboratory, Luleå, Sweden and analysed the day after. The laboratory is certified for all performed analyses. Analysed variables included concentrations of Al, As, Ba, Ca, Cd, Cl, Co, Cr, Cu, Hg, Fe, K, Mg, Mn, Mo, Na, Ni, P, Pb, S, Si, Sr, Ti, V, Zn, and N-tot. For our study, we focussed on the evaluation of Cd, Cu and Zn, which were the elements of highest environmental concern as known from former studies on the Vormbäcken system (Jacks et al. 2005; Samuelsson 2010; Sjöblom 2003). Concentrations of tot-N and P were used as explanatory variables. For Cd, Cu, and Zn no significant differences between samples from 2011 and 2012 were found in riparian vegetation and in vegetation from the river channel.

Table 3-1. Summary of dominating riparian species and species from the river channel that were sampled for chemical analyses in order of decreasing sampling frequency. The localities (Hornträsket, Ht, and L1 – L3) refer to the spatial gradient from the source of contamination and the belts (I-V) refer to the lateral distance of sampling points from the river channel (see also Material & Methods).

Species	Locality	Belt
Riparian zone		
<i>Carex rostrata/vesicaria</i>	Ht	I/II ¹
	L1, L2, L3	I-V
<i>Salix</i> sp.	Ht	I/II ¹
	L1, L3	I-V
	L2	III-V
<i>Eriophorum angustifolium</i>	L2, L3	II-V
<i>Carex nigra</i> ssp. <i>juncella</i>	L1	I-III
	L3	I
<i>Molinia caerulea</i>	L3	II-V
<i>Trichophorum cespitosum</i>	L3	II-V
<i>Betula nana</i>	L1	IV-V
River channel		
<i>Equisetum fluviatile</i>	Ht, L1, L2	
<i>Nuphar lutea</i>	Ht, L2, L3	
<i>Sparganium angustifolium</i>	L1, L2, L3	
<i>Potamogeton alpinus</i>	L1, L2	
<i>Hippuris vulgaris</i>	L2, L3	
<i>Potamogeton gramineus</i>	L3	

¹ in one sample

For the chemically analysed riparian species, biomass was sampled in July/August 2011 and July 2012, so that we had at least three samples per species and cover class. The above-ground living biomass of the species was taken from each sample plot (50 × 50 cm) and the weight was recorded. Most of the sample plots were also used for the determination of the total biomass (see above). The number of samples per cover class and species ranged from 3 – 28 (mean 8), except for *Betula nana* C2, which occurred in only two sample plots.

At each locality, samples for water chemistry were taken at five occasions 14 July – 2 August 2011. One additional sample was taken at each locality and at Hornträsket 24 July 2012. Samples were analysed the day after sampling (see above). Analysed variables included dissolved (<0.45 µm) concentrations of all elements analysed in vegetation (see above), except of Ti and V. In addition, NH₄-N, NO₃-N, NO₂-N, and TOC as well as chlorophyll content, alkalinity, conductivity, pH, colour and absorbance (420 nm) were analysed.

Within the environmental monitoring programme of Boliden Mineral AB (Boliden, Sweden), the operator of the Kristineberg mine, additional water samples were taken from Vormbäcken in 11 July 2011 at the outlet of Hornträsket, at Aspliden, at Brännfors, and at Vormsele, just before the confluence with Vindelälven.

Flow data for Vormbäcken modelled on a daily and monthly basis since 1990 were available from the Swedish Meteorological and Hydrological Institute (<http://vattenweb.smhi.se>). Flow data was divided into sub-catchments between the confluences of major tributaries of Vormbäcken. To calculate the flow for L1 – L3, we used the flow of the respective sub-catchment in which the locality was located.

3.4 Vegetation mapping

Vegetation mapping was done in a geographic information system using ArcGIS software (ESRI 2010) and was based on the high-resolution orthoimages acquired with the PAMS and the field data of species composition and cover in the sample plots and local knowledge derived by field visits (sensu Tempfli et al. 2009). Mapping was performed at a scale 1:100 with a minimum mapping area of 0.4 m². We delineated vegetation stands, i.e. units of homogenous areas that were characterized by defined species composition. Vegetation stands characterized by the same species composition belonged to the same vegetation class. The number of species characterizing a specific vegetation class ranged from 1-8. At each locality, we mapped a river stretch of 320 m length. We mapped non-submerged vegetation within the river channel and the entire riparian area within the littoral zone up to the forest layer including wetlands adjacent to the river (exemplified for L3 in Figure 3-4).

Mapping of the riparian area was divided into two steps. In a first step, the area where the sample plots were placed was mapped. All vegetation stands that intersected with the area where the sample plots were placed are from now on called the core zone (exemplified for L3 in Figure 3-2-3b). During field work in 2012 printouts of the mapped core zones were verified by walking through the core zone and comparing vegetation boundaries in the field with those on the map. In a second step, a preliminary map of the area around the core zone (from now on called extension zone) was made, based on the knowledge from the mapping of the core zone (see Figure 3-4 for the generated vegetation map at L3). Control points that were selected from the orthoimages ($n = 108$ at L1, $n = 87$ at L2, and $n = 63$ at L3) were visited in May, June and August 2012 to verify and adjust the map of the extension zones.

3.5 Biomass estimation

The biomass calculation for the study area was based on the total weight of the fresh biomass harvested from the sample plots (expressed as kg/m²). We calculated the biomass [kg] for each vegetation class by multiplying the vegetation class-specific mean biomass [kg/m²] with the area covered by the respective vegetation class. The vegetation class-specific mean biomass is the mean of all sample plots placed inside the vegetation class. For vegetation classes that only occurred in the extension zone, the vegetation class-specific mean biomass was taken from the vegetation class occurring inside the core zone of the respective locality which had the most species in common. If the number of species in common was the same for several vegetation classes, we took the mean biomass

of these classes. At locality L2, we identified multiple-species vegetation classes that occurred only in the extension zone and that had less than two species in common with core vegetation classes. For these vegetation classes, we used the biomass of the core vegetation class of another locality which had the most species in common. If the number of species in common was the same for several vegetation classes we took the mean biomass of these classes. For single-species vegetation classes that occurred only in the extension zone (*Carex rostrata/vesicaria* and *Salix* sp.) we took the biomass of the corresponding core vegetation class of another locality. The single-species vegetation class *Eriophorum angustifolium* (L2) was not represented in any core zone. In this case, we used the species-specific biomass of the highest observed cover class (C3). This procedure resulted in three levels of potential uncertainty: very low uncertainty for the core zone (23% of the total area), low uncertainty for areas in the extension zone which belonged to vegetation classes that also occurred within the core zone (extension zone I, 30% of the total area), and moderate uncertainty for areas that belonged to vegetation classes that only occur in the extension zone (extension zone II, 47% of the total area, Table 4-3). The biomass of trees >1.5 m was not included in the biomass estimation.

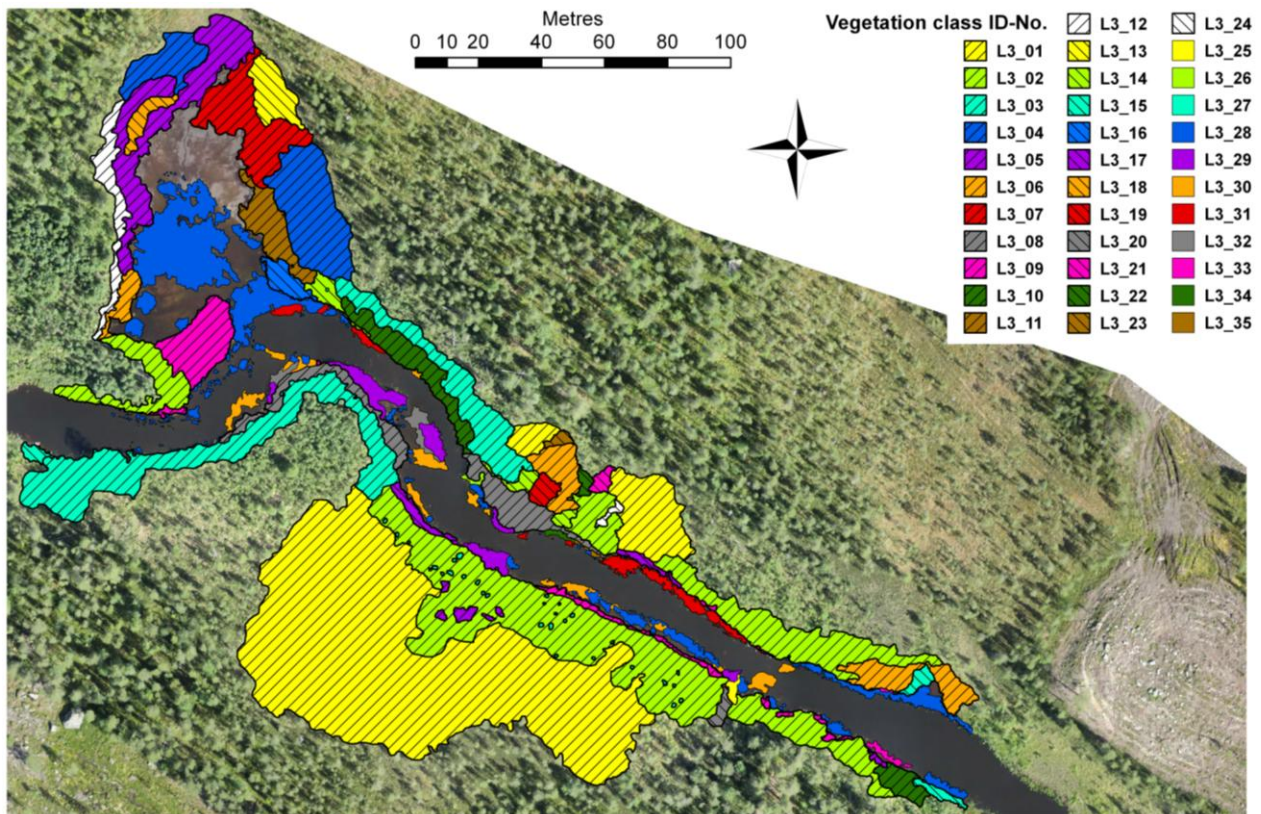


Figure 3-4. Vegetation map of non-submerged vegetation within the river channel and the entire riparian area within the littoral zone at L3.

3.6 Metal storage in vegetation

We calculated the amount of stored Cd, Cu and Zn in riparian vegetation based on the results of the chemical analysis, the species-specific biomass for each cover class (C1 – C4) and the areas for different vegetation classes obtained from vegetation mapping. We also took into account the spatial variation of species frequency and cover within each vegetation class. For the core and extension zone I, the amount M of metal x in species s at locality k [g] was calculated according to (1).

$$(1) \quad M_{x,s,L_k} = \sum_{i=1}^n r_{s,V_i} A_{V_i} b_{s,V_i} z_{x,s,L_k}$$

where r_{s,V_i} = frequency of species s within vegetation class i according to (2)
 A_{V_i} = area of vegetation class i [m²]

b_{s,V_i} = vegetation class-specific biomass of species s [kg/m²] according to (3)
 z_{x,s,L_k} = concentration of metal x in species s at locality k (mean of belts,
 see section 3.2) [g/kg]

$$(2) \quad r_{s,V_i} = \frac{n_{s,V_i}}{n_{V_i}}$$

where n_{s,V_i} = number of sample plots with species s in vegetation class i
 n_{V_i} = total number of sample plots in vegetation class i

$$(3) \quad b_{s,V_i} = \sum_{j=2}^4 n_{s,C_j,V_i} b_{s,C_j}$$

where n_{s,C_j,V_i} = number of sample plots with species s and cover class j in vegetation class i
 b_{s,C_j} = mean biomass of cover class j for species s [kg/m²].

The approach for the extension zone II was more generalized. Instead of vegetation class-specific information we used locality-specific information on species frequency and cover. The amount m of metal x in species s at locality k [g] was calculated according to (4).

$$(4) \quad m_{x,s,L_k} = r_{s,L_k} E_{s,L_k} b_{s,L_k} z_{x,s,L_k}$$

where r_{s,L_k} = frequency of species s at locality k (5)
 E_{s,L_k} = total area of vegetation classes in extension zone II that contain species s at locality k [m²]
 b_{s,L_k} = locality-specific biomass of species s [kg/m²] according to (6)
 z_{x,s,L_k} = concentration of metal x in species s at locality k (mean of belts,
 see section 3.2) [g/kg]

$$(5) \quad r_{s,L_k} = \frac{n_{s,L_k}}{n_{L_k}}$$

where n_{s,L_k} = number of sample plots with species s at locality k
 n_{L_k} = total number of sample plots at locality k

$$(6) \quad b_{s,L_k} = \sum_{j=2}^4 n_{s,C_j,L_k} b_{s,C_j}$$

where n_{s,C_j,L_k} = number of sample plots with species s and cover class j at locality k
 b_{s,C_j} = mean biomass of cover class j for species s [kg/m²].

3.7 Assessment of biodiversity

To assess the biodiversity of vegetation at each locality, we calculated a) species richness, b) Shannon's index of diversity and c) Shannon's evenness index. All indices are frequently used in biodiversity studies, but might refer to different aspects of diversity (Heip & Engels 1974; Cousins 1991). Species richness gives the number of species per locality. Shannon's index of diversity, in contrast to Simpson's index takes also into account the occurrence of rare species (Smith & Smith 2006). Shannon's evenness index rescales the Shannon index so that it ranges between 0 and 1, where 0 refers to localities with only one species and the index approaches 0 as the frequency distribution among the species becomes increasingly uneven (i.e., dominated by 1 species). Evenness = 1 when distribution of frequency among species is perfectly even (i.e., proportional frequencies are the same) (McGarigal 1995).

3.8 *Statistical analysis*

We performed non-metric Mann-Whitney U and Kruskal-Wallis tests for comparisons between two groups and multiple groups, respectively. Groups with $n < 3$ were excluded. We used three significance levels ($p = 0.05, 0.01$ and 0.001). When the Kruskal-Wallis test indicated a significant difference between at least two of the compared groups, we used Multiple Comparisons to compute post-hoc comparisons of mean ranks of all pairs of groups to identify the group differences that were significant. For group comparisons we used the Statistica software (StatSoft Inc. 2011). To identify general patterns of relationship between metal concentrations in water, vegetation from the river channel and riparian vegetation we performed non-metric Multidimensional Scaling (MDS) with PAST software (Hammer et al. 2001) using the Rho similarity measure (based on Spearman's correlation coefficient of ranks, with column average substitution for missing data). Only species occurring at ≥ 3 localities (including Hornträsket) were included.

4 RESULTS

4.1 Water chemistry

Concentrations of Cd, Cu and Zn decreased with increased distance from Horsträsket (Figure 4-1). According to the standards of the Swedish Environmental Protection Agency (1999), Cd and Cu concentrations ranged from high to moderate and Zn concentrations ranged from very high to moderate (Figure 4-1). The concentrations along Vormbäcken showed the same pattern in 2011 and 2012 (Figure 4-1). However, due to differences in precipitation, the flow in July 2012 was about two fold the flow in July 2011 (1.91 and 1.01 m³/s, respectively, at L3). This resulted in lower concentrations in 2012 compared to 2011 (Figure 4-1), except for Cu at L3. Throughout the sampling period in 2011, flow variation was low (mean 0.90 ± 0.03 m³/s, range 0.84 – 0.94 m³/s at L3). Therefore we treated the five samples taken in 2011 as replicates. Concentrations at L1 in 2011 were significantly different from concentrations at L3 for all three elements (Cd: $H_{2, N=15} = 12.50$, $p < 0.01$, $p_{L1-L3} < 0.01$; Cu: $H_{2, N=15} = 12.52$, $p < 0.01$, $p_{L1-L3} < 0.01$; Zn: $H_{2, N=15} = 12.52$, $p < 0.01$, $p_{L1-L3} < 0.01$; Figure 4-1a – c). Zn concentrations in 2011 increased between Aspliden and L1 (Figure 4-1c). N-tot concentrations in Vormbäcken decreased from 0.66 mg/l at L1 to 0.57 mg/l at L2 and 0.42 mg/l at L3 in July/August 2011 ($n = 5$). The aquatic system was P limited, i.e. N:P > 23 (Wetzel 2001), with mean N:P ratios of 160, 121, and 79 at L1 – L3, respectively.

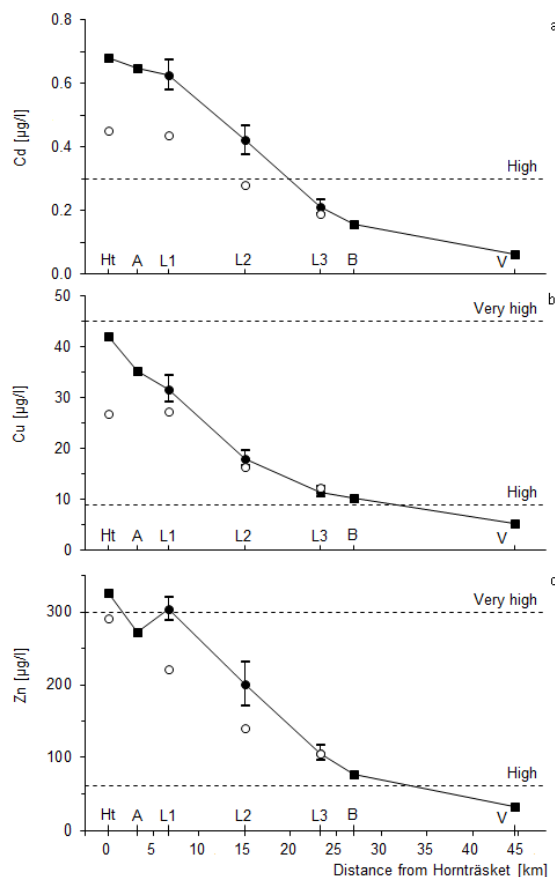


Figure 4-1. Cd, Cu and Zn concentrations \pm SD in Vormbäcken in July/August 2011 and in July 2012 as a function of distance from Horsträsket (Ht). In 2011, samples at the outlet of Horsträsket, Aspliden (A), Brännfors (B) and Vormsele (V) were taken by Boliden Mineral AB (\blacksquare , $n = 1$), samples at L1 – L3 were taken by the authors (\bullet , $n = 5$); in 2012 samples were taken by the authors (\circ , $n = 1$). Horizontal dashed lines represent standard values of the Swedish Environmental Protection Agency (1999) for the assessment of metal contents in lakes and minor water courses.

Assuming the concentrations of Cd, Cu and Zn being constant throughout the growing season (middle of Mai – End of August) which is supported by Sjöblom (2003), the total amount of Cd, Cu and Zn transported by Vormbäcken within this time span in 2011 ranged from 3.7 kg for Cd at L1 to 2193 kg for Zn at L3 (Table 4-1).

Table 4-1. Amount [kg] of Cd, Cu, and Zn transported by Vormbäcken during the growing season in 2011 at L1 – L3.

Element	L1	L2	L3
Cd	3.7	4.6	4.4
Cu	187.2	195.8	237.4
Zn	1799.2	2181.5	2193.5

4.2 Vegetation chemistry

Concentrations of Cd, Cu, and Zn in riparian vegetation did not differ between belts, neither in combined species nor single species (*Carex rostrata/vesicaria* belt I – V, *Salix* sp. belt III – V) analyses. However, Cu concentrations combined for all species showed a decreasing trend with increasing distance from the river (Figure 4-2-1). In further analysis samples from different belts were treated as replicates.

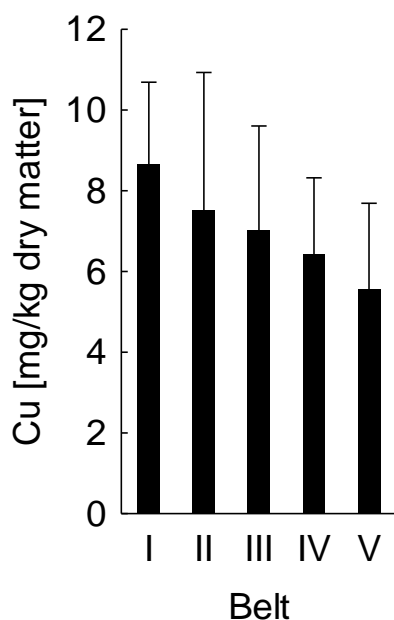


Figure 4-2-1. Mean plot + SD of Cu concentrations in riparian vegetation in belt I-V ($n = 7$ in belt I, $n = 10$ in belt II, and $n = 11$ in belt III – V).

Combining all species, concentrations of Cd, Cu, and Zn in riparian vegetation were lower at L3 than at L1 (Figure 4-2-2 – 4-2-4), but differences between localities were only significant for Cu L1 – L3 and L2 – L3 ($H_{2, N=50} = 13.27$, $p < 0.01$, $p_{L1-L3} < 0.01$, $p_{L2-L3} < 0.05$). Single species analyses showed

no significant differences between localities. Concentrations in *Carex rostrata/vesicaria* and *Salix* sp. behaved differently at locality L1 and L3 (*C. rostrata/vesicaria* L1 < L3 and *Salix* L1 > L3 for all elements, Figure 4-2-2 – 4-2-4).

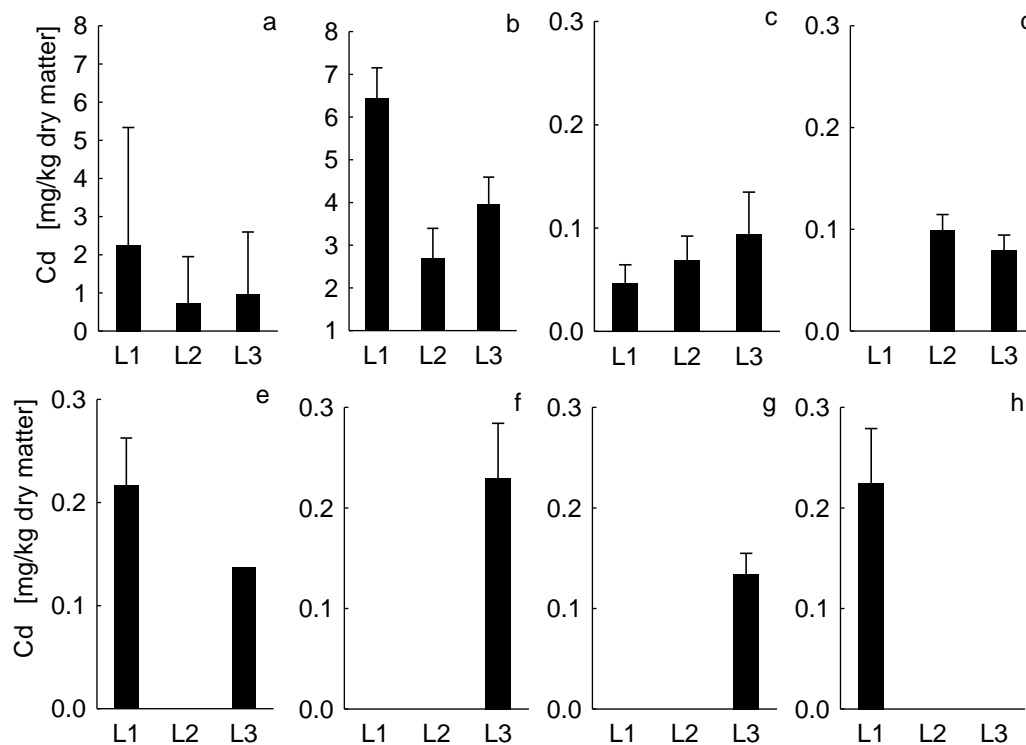


Figure 4-2-2. Mean plots + SD of Cd concentrations in riparian vegetation at L1 – L3: a) combined species ($n = 15, 12,$ and 23 at L1, L2, and L3, respectively); b) *Salix* sp. ($n = 5$ at L1 and L3, $n = 3$ at L2); c) *Carex rostrata/vesicaria* ($n = 5$); d) *Eriophorum angustifolium* ($n = 4$); e) *Carex nigra* ssp. *juncella* ($n = 3$ at L1, $n = 1$ at L3); f) *Molinia caerulea* ($n = 4$); g) *Trichophorum cespitosum* ($n = 4$); h) *Betula nana* ($n = 2$).

Concentrations of Cd, Cu, and Zn in riparian vegetation varied among species. *Salix* sp. contained most Cd and Zn at all localities. Most pronounced was the difference between *Salix* sp. and *Carex rostrata/vesicaria*, which was significant in 5 of 9 cases: Cd at L1, L2, and L3 (L1: $H_{2, N=13} = 10.55$, $p < 0.01$, $p_{Salix-C.rostrata/vesicaria} < 0.01$; L2: $H_{2, N=12} = 7.93$, $p < 0.05$, $p_{Salix-C.rostrata/vesicaria} < 0.05$; L3: $H_{4, N=22} = 18.10$, $p < 0.01$, $p_{Salix-C.rostrata/vesicaria} < 0.01$) and Zn at L1 and L2 (L1: $H_{2, N=13} = 10.55$, $p < 0.01$, $p_{Salix-C.rostrata/vesicaria} < 0.01$; L2: $H_{2, N=12} = 8.45$, $p < 0.05$, $p_{Salix-C.rostrata/vesicaria} < 0.05$). *Salix* sp. differed also from *Eriophorum angustifolium* for Cd at L3 ($p_{Salix-E.angustifolium} < 0.01$) and from *Molinia caerulea* and *Trichophorum cespitosum* for Zn at L3 ($H_{4, N=22} = 14.44$, $p < 0.01$, $p_{Salix-M.caerulea} < 0.05$, $p_{Salix-T.cespitosum} < 0.05$). Another significant difference was *Carex rostrata/vesicaria* – *Carex nigra* ssp. *juncella* for Cu at L1 ($H_{2, N=13} = 9.92$, $p < 0.01$, $p_{C.rostrata/vesicaria-C.nigra} < 0.01$). Combined for all localities (including Horotrasket) concentrations of Cu were higher in vegetation from the river channel than in riparian vegetation that occurred in belt I ($U_{n_1=34, n_2=14} = 4$, $p < 0.001$). Combined for all species, Cd, Cu and Zn concentrations in river channel vegetation did not differ between localities. Combined for all localities, only *Equisetum fluviatile* and *Nuphar lutea* differed for Cd ($H_{2, N=9} = 6.49$, $p < 0.05$, $p_{E.fluviatile-N.lutea} < 0.05$).

MDS combined for all localities (including Horotrasket) showed that the mean concentrations of Cd, Cu and Zn were more similar between riparian vegetation and water than between riparian vegetation and vegetation from the river channel (Figure 4-6). The Shepard plot indicated good MDS results (stress: 0.03, R^2 axis 1: 0.68, R^2 axis 2: 0.17).

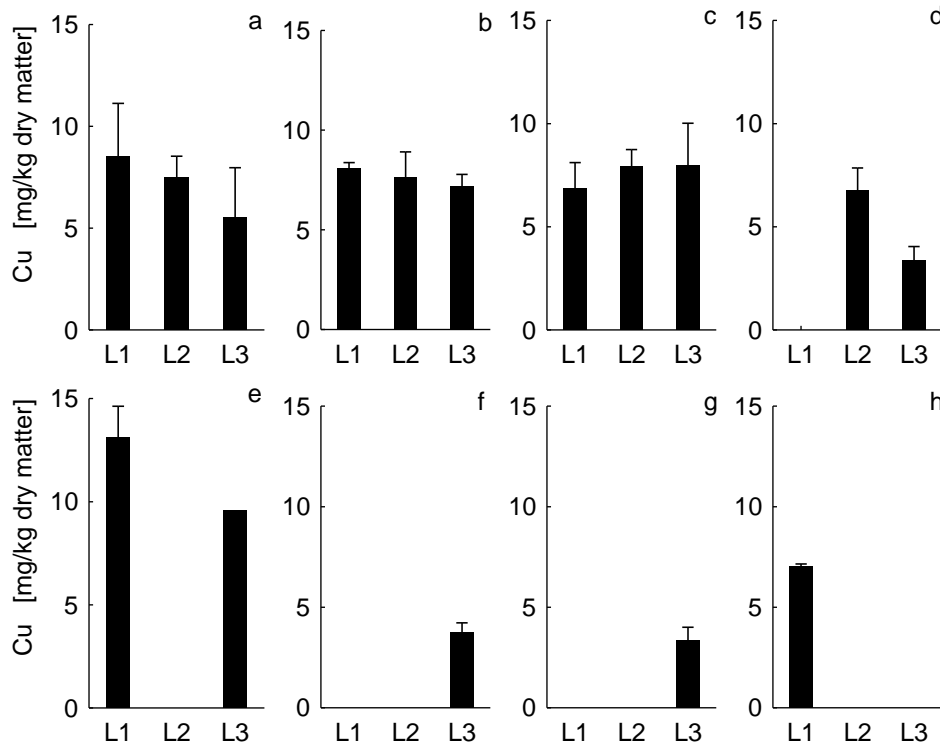


Figure 4-2-3. Mean plots + SD of Cu concentrations in riparian vegetation at L1 – L3: a) combined species (n = 15, 12, and 23 at L1, L2, and L3, respectively); b) *Salix* sp. (n = 5 at L1 and L3, n = 3 at L2); c) *Carex rostrata/vesicaria* (n = 5); d) *Eriophorum angustifolium* (n = 4); e) *Carex nigra ssp. juncella* (n = 3 at L1, n = 1 at L3); f) *Molinia caerulea* (n = 4); g) *Trichophorum cespitosum* (n = 4); h) *Betula nana* (n = 2).

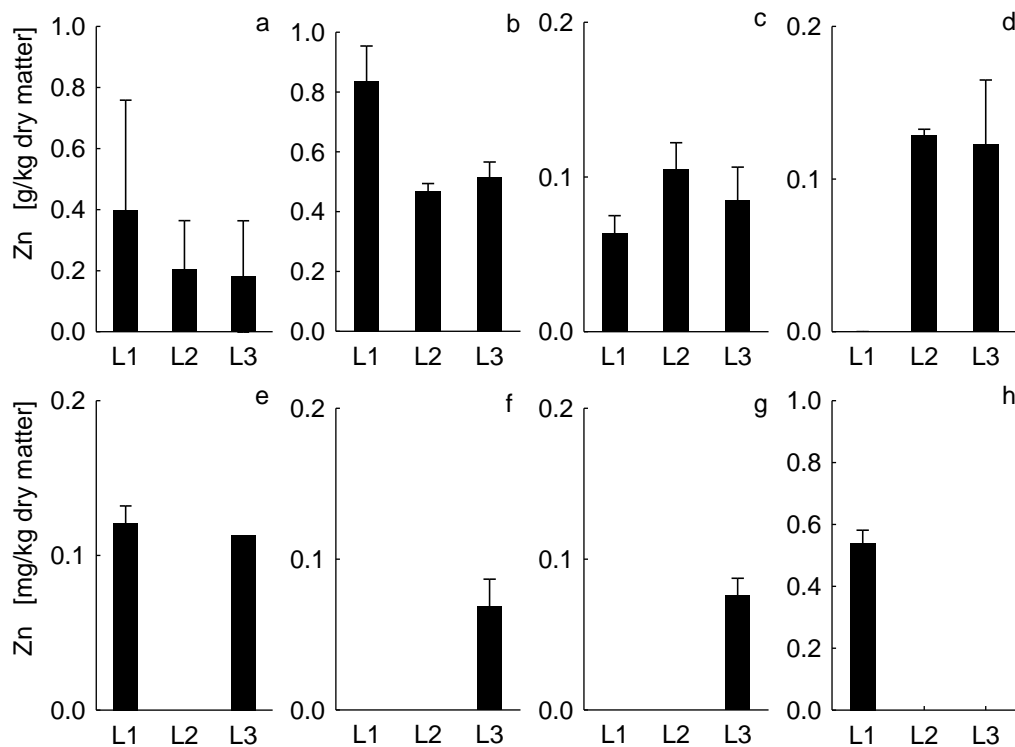


Figure 4-2-4. Mean plots + SD of Zn concentrations in riparian vegetation at L1 – L3: a) combined species (n = 15, 12, and 23 at L1, L2, and L3, respectively); b) *Salix* sp. (n = 5 at L1 and L3, n = 3 at L2); c) *Carex rostrata/vesicaria* (n = 5); d) *Eriophorum angustifolium* (n = 4); e)

Carex nigra ssp. *juncella* ($n = 3$ at L1, $n = 1$ at L3); f) *Molinia caerulea* ($n = 4$); g) *Trichophorum cespitosum* ($n = 4$); h) *Betula nana* ($n = 2$).

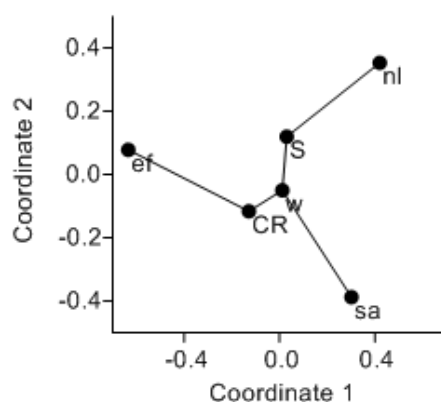


Figure 4-2-5. Multidimensional Scaling diagram with minimum span tree of metal concentrations (Cd, Cu and Zn combined) in water (w), riparian vegetation (*Carex rostrata/vesicaria*, CR and *Salix* sp., S) and vegetation from the river channel (*Equisetum fluviatile*, ef, *Nuphar lutea*, nl, and *Sparganium angustifolium*, sa).

4.3 Area of vegetation classes and vegetation biomass

At L1, the size of the mapped riparian area was 1.3 ha (Table 4-3). The area was composed of 31 vegetation classes of which 12 were represented within the core zone (Appendix I). The three vegetation classes with the largest area were L1_1: *Betula pubescens*, *Calamagrostis canescens*, *Carex nigra*, *Carex nigra* ssp. *juncella*, *Carex rostrata/vesicaria*, *Molinia caerulea*, *Salix* sp. (0.21 ha), L1_2: *Alnus incana* ssp. *incana*, *Betula nana*, *B. pubescens*, *C. canescens*, *C. nigra* ssp. *juncella*, *C. rostrata/vesicaria* (0.12 ha), and L1_3: *B. pubescens*, *C. canescens*, *Calamagrostis purpurea*, *C. nigra* ssp. *juncella*, *Salix* sp. (0.12 ha, Appendix I).

Table 4-3. Area (A) and biomass (Bm) of core zone and extension zones I and II at Locality L1, L2, and L3.

	Core zone			Extension zone I			Extension zone II			Total		
	A [ha]	Bm [t]	[t/ha]	A [ha]	Bm [t]	[t/ha]	A [ha]	Bm [t]	[t/ha]	A [ha]	Bm [t]	[t/ha]
L1	0.2	1.9	8.5	0.1	2.5	19.4	1.0	7.9	8.2	1.3	12.2	9.4
L2	1.0	7.2	7.5	0.7	6.1	8.5	1.3	8.9	7.1	2.9	22.2	7.5
L3	0.2	1.3	5.8	1.0	4.5	4.7	0.7	3.8	5.8	1.8	9.6	5.2
Total	1.4	10.3	7.4	1.8	13.1	7.3	2.9	20.5	7.2	6.1	44.0	7.2

At L2, the size of the mapped riparian area was 3.0 ha (Table 4-3). The area was composed of 12 vegetation classes of which two were represented within the core zone (Appendix I). The three vegetation classes with the largest area were L2_1: *C. rostrata/vesicaria*, *E. angustifolium* (1.20 ha), L2_2: *C. rostrata/vesicaria*, *E. angustifolium*, *Salix* sp. (0.54 ha), and L2_3: *C. rostrata/vesicaria* (0.48 ha, Appendix I).

At L3, the size of the mapped riparian area was 1.8 ha (Table 4-3). The area was composed of 27 vegetation classes of which ten were represented within the core zone (Appendix I). The three vegetation classes with the largest area were L3_1: *A. polifolia*, *B. pubescens*, *E. angustifolium*, *M.*

caerulea, *Pinus sylvestris*, *T. cespitosum* (0.64 ha), L3_2: *B. pubescens*, *C. nigra*, *C. nigra* ssp. *juncella*, *E. angustifolium*, *M. caerulea*, *Salix* sp. (0.39 ha), and L3_3: *B. pubescens*, *C. canescens*, *C. nigra* ssp. *juncella*, *M. caerulea*, *Pinus sylvestris*, *Salix* sp. (0.19 ha, Appendix I).

L1 was the most productive locality (Table 4-3) with 9.4 t/ha, followed by L2 (7.5 t/ha) and L3 (5.2 t/ha).

4.4 Metal storage in and biomass of dominating riparian species

The total amount of stored Cd, Cu and Zn in the dominating species of the riparian vegetation was 1041, 6986, and 208852 g, respectively (Table 4-4-1). The total amount of Cd and Zn decreased with increasing distance from the source of contamination (Table 4). The maximum amount of Cu was stored at L2 (Table 4-4-1). *Salix* sp. contained 94% of all Cd and 63% of all Zn, but only 15% of the total biomass. *Carex rostrata/vesicaria* contained 74% of all Cu and 74% of the total biomass. Most Cd and Zn were accumulated at L1, where *Salix* sp. contributed 100 and 96% of the total amounts, respectively, and 67% of the total biomass. *Salix* sp. contributed 75% of the total Cu content at L1. Most Cu was accumulated at L2, where *Carex rostrata/vesicaria* contributed 96% of the total Cu amount and 94% of the total biomass. *Carex rostrata/vesicaria* contributed 93 and 94% of the total Cd and Zn content, respectively, at L2. At L3, *Molinia caerulea* contained most Cd while *Carex nigra* ssp. *juncella* contained most Cu and Zn (Table 4-4-1). At L3, *Salix* sp. was not among the dominating species, but biomass and contents of Cd, Cu and Zn largely exceeded (up to 4470 fold for Cd) the total metal amount stored in the dominating species (Table 4-4-1).

Table 4-4-1 Biomass (Bm) and amount of stored Cd, Cu and Zn in dominating riparian species. Species are listed in order of decreasing number of belts in which they were dominating (n). *Salix* sp. at L2 and L3 is included for comparison.

Species	n	Bm [t]	Cd [g]	Cu [g]	Zn [g]
L1					
<i>Salix</i> sp.	4	285.3	983.3	1218.6	130790.5
<i>Betula nana</i>	2	6.2	0.8	25.9	1968.3
<i>Carex nigra</i> ssp. <i>juncella</i>	2	11.0	1.5	91.4	857.4
<i>Carex rostrata/vesicaria</i>	2	124.1	1.9	279.4	2623.8
Sub-total L1		426.5	987.5	1615.3	136240.0
L2					
<i>Carex rostrata/vesicaria</i>	5	1279.8	42.2	4861.5	64455.1
<i>Eriophorum angustifolium</i>	4	75.8	3.1	211.8	4010.6
Sub-total L2		1355.6	45.2	5073.3	68465.7
L3					
<i>Carex rostrata/vesicaria</i>	4	22.0	0.8	65.9	699.1
<i>Eriophorum angustifolium</i>	4	13.5	0.5	19.8	730.1
<i>Molinia caerulea</i>	4	61.3	4.8	76.4	1405.4
<i>Trichophorum cespitosum</i>	4	3.3	0.1	3.4	76.4
<i>Carex nigra</i> ssp. <i>juncella</i>	1	25.9	2.3	147.1	1473.5
Sub-total L3		126.1	8.6	312.5	4384.5
Total		1908.2	1041.3	7001.1	209090.2
<i>Salix</i> sp. L2 ¹		42.2	46.1	130.3	8008.6
<i>Salix</i> sp. L3 ¹		21880.9	38270.2	69110.7	4963398.5

¹ not dominating

Compared to the total amount of Cd, Cu, and Zn transported by Vormbäcken during the growing season at L1, L2, and L3, riparian vegetation stored at a maximum 26.7% of Cd (L1), 3.1% of Cu (L3), and 7.6% of Zn (L1, Table 4-4-2).

Table 4-4-2. Proportion [%] of Cd, Cu and Zn stored in riparian vegetation at L1 – L3 compared to the total amount transported by the water of Vormbäcken during the growing season.

Element	Locality		
	L1	L2	L3
Cd	26.7	1.0	0.2
Cu	0.9	2.6	0.1
Zn	7.6	3.1	0.2

4.5 Biodiversity

There was no consistent trend in the change of plant diversity along Vormbäcken. Plant diversity was lowest at locality L2, irrespective of diversity index, and didn't differ between L1 and L3 (Figure 4-5). At most, there were 23 plant species (locality L3). At locality L2, there were in total only six plant species and two of the studied belts included only two species of which *Carex rostrata/vesicaria* was present in both belts.

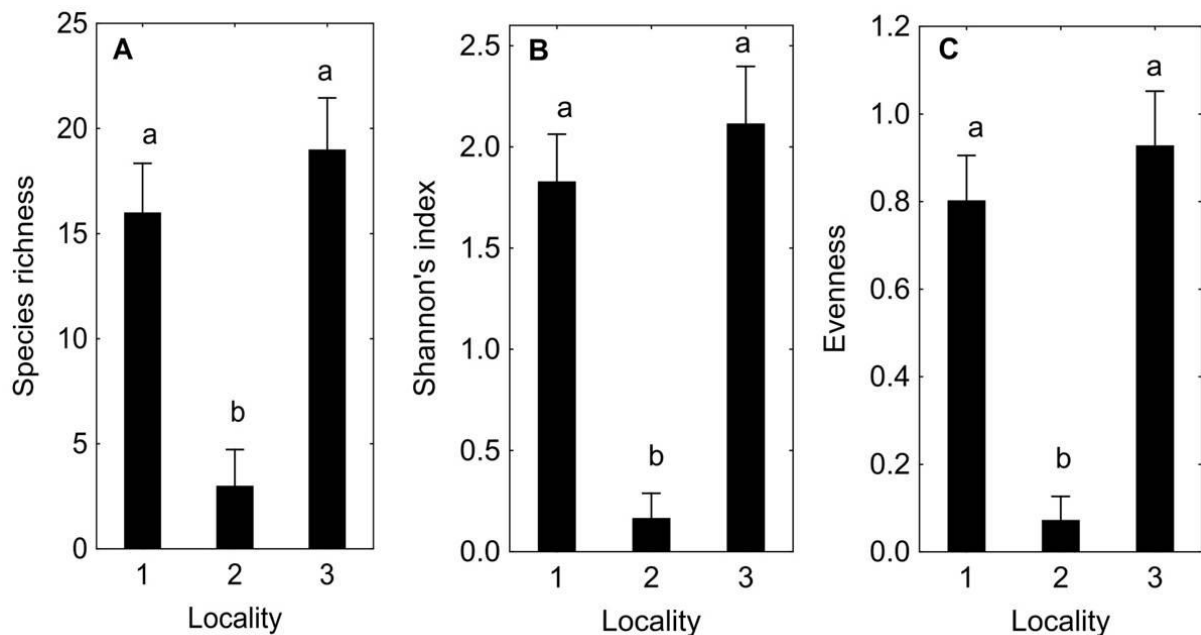


Figure 4-5. Biodiversity along the three localities at Vormbäcken. Diversity was calculated per belt. Different letters indicate significant differences in diversity ($p < 0.01$).

5 DISCUSSION

The observed pattern of decreasing metal concentrations in the river water with increased distance from Hornträsket is in accordance with former studies on Vormbäcken (Sjöblom 2003). Due to differences in the sampling procedure and dates between sampling by the authors and by Boliden Mineral AB, there might be inconsistency in the data, which could explain the increasing Zn concentrations between Aspliden and L1. In contrast to water, Cd and Zn concentrations in neither vegetation from the river channel, nor riparian vegetation decreased significantly with increased distance from the source of contamination (Hornträsket). However, both metals showed their maximum concentration in riparian vegetation at L1. Also the total amount of Cd and Zn in riparian vegetation decreased from L1 to L3. This shows that the decreasing Cd and Zn concentrations in the water of Vormbäcken along the spatial gradient had a higher impact on riparian vegetation than on vegetation from the river channel. This is also supported by the result of MDS. Concentrations of Cu in riparian vegetation decreased significantly with increased distance from the source of contamination and showed a decreasing trend with increasing distance from the river, but most vegetation-bound Cu was found at L2. In addition, Cu concentrations were found to be higher in vegetation from the river channel than in riparian vegetation. This shows that Cu behaved differently from Cd and Zn. As for terrestrial plants, the metal accumulation in rooted vascular aquatic plants is ruled by metal concentrations in the substrate (Jackson 1998). Therefore it is difficult to draw conclusions on the influence of dissolved metals in the water on metal contents in vegetation without studying concentrations in the particulate fraction and the sediment/soil.

The flexibility of the used UAS (transportable and operable by a single person) permitted to carry out remote sensing exactly at the desired location and time, without being dependent on external image providers. The sub-decimetre resolution (5 cm) of the produced orthoimages allowed for detailed vegetation classification and mapping with high accuracy (Husson et al., manuscript) throughout the entire riparian zone. It was possible by visual interpretation to delineate vegetation stands on the images and to relate the specific optical appearance of the stands to species compositions derived from field visits, including tree, shrub, and herbaceous species as well as non-submerged aquatic species. Because of the narrow spatial extend of riparian zones (often < 30 m), high spatial resolution has been found to be the main feature to improve riparian vegetation classification (Goetz 2006; Muller 1997). Previous remote sensing approaches on riparian vegetation have so far not been able to resolve herbaceous and shrub vegetation at the species level which is mainly due to the spatial resolution of available remote sensing data or limitations in automated image classification. So far discrimination was successful between several land cover/use classes like e.g. agriculture, forest, grass, and shrub (Forzieri et al. 2010; Lattin et al. 2004; Schuft et al. 1999; Tormos et al. 2011), between a small number of tree/shrub species, including invaders (Dunford et al. 2009; Frazier and Wang 2011; Hamada et al. 2007; Lonard et al. 2000; Nagler et al. 2009; Nagler et al. 2005; Petersen et al. 2005) and for single invasive herbaceous species (Andrew and Ustin 2009; Hestir et al. 2008). Our study demonstrated that plant species differ significantly in their uptake of trace elements (see also Pilon-Smits 2005; Pugh et al. 2002; Vandecasteele et al. 2002). In addition, the here studied vegetation stands were generally characterized by multiple species. Single-species stands occurred mainly at locality L2. Biomass assessments with remote sensing using satellite images with varying spatial resolution (30 – 1 m) have successfully been applied to large-scale single-species stands in wetlands (e.g. Gross et al. 1987, reviewed by Ozesmi and Bauer 2002), and for the assessment of total wetland biomass (Mutanga et al. 2012 as well as Proisy et al. 2007, Rendong and Jiyuan 2004, and Tan et al. 2003, reviewed by Adam et al. 2010). Applying such traditional remote sensing with satellite images to the here studied riparian zones would however miss the high spatial variation in vegetation stands, biomass and trace element uptake. The here presented method is suited for a more accurate assessment in terms of vegetation class- and species-specific biomass and trace element contents. This allows for detailed modelling of nutrient and trace element cycling in the riparian zone and of interactions with the adjacent aquatic system. Compared to the large spatial extensions covered by the satellite-based wetland studies (6 – 3000 km²), the reach of our method is limited to river stretches of several hundreds of meters length. Two main reasons for this limitation were detected: a) increasing potential uncertainty with increasing distance from the core zone and b) the duration of visual image

interpretation and field sampling necessary to train the interpreter and for biomass determination. The first reason applies to areas with large spatial variation in vegetation. This variation leads to the occurrence of vegetation classes with species compositions that differ from those of any core zone vegetation class. This could however be redressed by distributing the sample plots over a larger area. To make field work more efficient, it could be divided into two steps. In a first step species composition and cover could be investigated as a basis for the vegetation mapping. After the validation of the vegetation map, biomass could be sampled by (randomly) selecting a certain number of points within each vegetation class, thereby reducing the total amount of samples. However, samples would then be distributed over a larger area, increasing the time necessary for sampling.

Biodiversity and species composition of vegetation appeared to be unaffected by potential contaminants in Vormbäcken. The low diversity of locality L2 is probably due to topography. This locality is rather flat and hence probably more regularly flooded compared to the other two localities. Regular flooding results in the exclusion of plant species otherwise found in the riparian zone, e.g. *Molinia caerulea*, *Calamagrostis canescens* and *Andromeda polifolia*.

For the planning of phytoremediation measures it is crucial to know to which extent contaminants accumulate in different plant species. Compared to the total amount of Cd, Cu, and Zn transported by Vormbäcken during the growing season at L1, L2, and L3, riparian vegetation stored at a maximum 26.7% of Cd (L1), 3.1% of Cu (L3), and 7.6% of Zn (L1, Table 4-4-2). Thus the harvesting of riparian vegetation before senescence, to avoid the release of the accumulated metals to the water could considerably reduce the burden of metals in Vormbäcken. Our study revealed that especially the removal of *Salix* sp. at L1 would be an efficient way to remove most of the vegetation-bound Cd and Zn but also a considerable amount of Cu from the system. Similar results on the potential of *Salix* sp. to extract Cd and Zn from contaminated soils were found by Vandecasteele (2002) as well as Klan-Westin and Eriksson (2003). The application of UAS in addition to field sampling for riparian vegetation monitoring has large potential to improve the accuracy of assessments of biomass and trace element/nutrient content at the scale of entire riparian zones.

6 ACKNOWLEDGEMENTS

We thank Olle Hagner from SmartPlanes AB for help with the aerial survey and Proper English AB for improving the English.

7 REFERENCES

- Adam, E., Mutanga, O., & Rugege, D. (2010). Multispectral and hyperspectral remote sensing for identification and mapping of wetland vegetation: a review. *Wetlands Ecology and Management*, 18(3), 281-296.
- Andrew, M., & Ustin, S. (2009). Habitat suitability modelling of an invasive plant with advanced remote sensing data. *Diversity & distributions*, 15(4), 627-640.
- Bishop, K., Lee, Y. H., Pettersson, C., & Allard, B. (1995). Terrestrial sources of methylmercury in surface waters - The importance of the riparian zone in the Svartberget Catchment. *Water Air and Soil Pollution*, 80(1-4), 435-444.
- Brånin, B., Söderström, O. & Backlund, S. (1976): Ekologiska effekter av en sulfidmalmgruvindustris utsläpp i ett vattensystem. Kristinebergsrecipienten, Västerbottens län. SNV PM 755. Statens naturvårdsverk, Solna, Sweden, 133 pp. (in Swedish, English summary).
- Bryson, M., Reid, A., Ramos, F., & Sukkarieh, S. (2010). Airborne vision-based mapping and classification of large farmland environments. *Journal of Field Robotics*, 27(5), 632-655.
- Cousins, S.H. (1991) Species diversity measurement: choosing the right index. *Trends in Ecology and Evolution*, 6, 190-192.
- Dunford, R., Michel, K., Gagnage, M., Piegay, H., & Tremelo, M. L. (2009). Potential and constraints of Unmanned Aerial Vehicle technology for the characterization of Mediterranean riparian forest. *International Journal of Remote Sensing*, 30(19), 4915-4935.
- ESRI (2010). ArcGIS 10.0. Redlands, CA.
- EU (2000). Directive 2000/60/EC of the European Parliament and of the Council of 23 October 2000 establishing a framework for Community action in the field of water policy. *Official Journal of the European Communities (Vol. L-327/1): EU (European Union)*.
- Forzieri, G., Moser, G., Vivoni, E., Castelli, F., & Canovaro, F. (2010). Riparian Vegetation Mapping for Hydraulic Roughness Estimation Using Very High Resolution Remote Sensing Data Fusion. *Journal of hydraulic engineering*, 136(11), 855-867.
- Frazier, A. E., & Wang, L. (2011). Characterizing spatial patterns of invasive species using sub-pixel classifications. *Remote Sensing of Environment*, 115(8), 1997-2007.
- Gibson, D. J. (2002). *Methods in comparative plant population ecology*. New York: Oxford University Press.
- Goetz, S. J. (2006). Remote sensing of riparian buffers: Past progress and future prospects. *Journal of the American Water Resources Association*, 42(1), 133-143.
- Gross, M. F., Hardisky, M. A., Klemas, V., & Wolf, P. L. (1987). QUANTIFICATION OF BIOMASS OF THE MARSH GRASS SPARTINA-ALTERNIFLORA LOISEL USING LANDSAT THEMATIC MAPPER IMAGERY. *Photogrammetric Engineering and Remote Sensing*, 53(11), 1577-1583.
- Hamada, Y., Stow, D. A., Coulter, L. L., Jafolla, J. C., & Hendricks, L. W. (2007). Detecting Tamarisk species (*Tamarix* spp.) in riparian habitats of Southern California using high spatial resolution hyperspectral imagery. *Remote Sensing of Environment*, 109(2), 237-248.
- Hammer, O., Harper, D. A. T., & Ryan, P. D. (2001). PAST 2.16.
- Haycock, N. E., Pinay, G., & Walker, C. (1993). Nitrogen-retention in river corridors: European perspective. *Ambio*, 22(6), 340-346.
- Heip, C. & Engels, P. (1974) Comparing Species Diversity and Evenness Indices. *Journal of the Marine Biological Association of the United Kingdom*, 54, 559-563.

- Hestir, E., Khanna, S., Andrew, M., Santos, M., & Viers, J. (2008). Identification of invasive vegetation using hyperspectral remote sensing in the California Delta ecosystem. *Remote Sensing of Environment*, 112(11), 4034-4047.
- Holmström, H., Salmon, U.J., Carlsson, E., Petrov, P. & Öhlander, B. (2001): Geochemical investigations of sulphide-bearing tailings at Kristineberg, northern Sweden, a few years after remediation. *The Science of the Total Environment* 273:111-133.
- Jacks, G., Lövgren, L., Löfgren, O., & Miskovsky, K. (2005). Study of the chemical and ecological status of Lake Hornträsket, mining district of Kristineberg, Northern Sweden. Paper presented at the International conference on mining and the environment, metals and energy recovery, Skellefteå, 27 June - 1 July 2005.
- Jackson, L. J. (1998). Paradigms of metal accumulation in rooted aquatic vascular plants. *Science of the Total Environment*, 219(2-3), 223-231.
- Jongman, R.H.G., ter Braak, C.J.F., van Tongeren, O.F.R., 1995. *Data analysis in community and landscape ecology*. Cambridge University Press, Cambridge.
- Kalff, J. (2001). *Limnology*. Upper Saddle River, NJ: Prentice Hall.
- Klang-Westin, E., & Eriksson, J. (2003). Potential of *Salix* as phytoextractor for Cd on moderately contaminated soils. *Plant and Soil*, 249(1), 127-137.
- Lattin, P. D., Wigington, P. J., Moser, T. J., Peniston, B. E., Lindeman, D. R., & Oetter, D. R. (2004). Influence of remote sensing imagery source on quantification of Riparian land cover/land use. *Journal of the American Water Resources Association*, 40(1), 215-227.
- Lonard, R. I., Judd, F. W., Everitt, J. H., Escobar, D. E., & Davis, M. R. (2000). Evaluation of color-infrared photography for distinguishing annual changes in riparian forest vegetation of the lower Rio Grande in Texas. *Forest Ecology and Management*, 128(1-2), 75-81.
- Mander, U., & Shirmohammadi, A. (2008). Transport and retention of pollutants from different production systems. *Boreal Environment Research*, 13(3), 177-184.
- McGarigal, K. & Marks, B.J. (1995) FRAGSTATS: spatial pattern analysis program for quantifying landscape structure. General Technical Report (PNR-GTR-351), US Department of Agriculture, Forest Service, 351.
- Mueller-Dombois, D., & Ellenberg, H. (2002). *Aims and methods of vegetation ecology*. New York: Wiley & Sons.
- Muller, E. (1997). Mapping riparian vegetation along rivers: old concepts and new methods. *Aquatic Botany*, 58(3-4), 411-437.
- Mutanga, O., Adam, E., & Cho, M. (2012). High density biomass estimation for wetland vegetation using WorldView-2 imagery and random forest regression algorithm. *International journal of applied earth observation and geoinformation*, 18, 399-406.
- Nagler, P. L., Glenn, E. P., & Hinojosa-Huerta, O. (2009). Synthesis of ground and remote sensing data for monitoring ecosystem functions in the Colorado River Delta, Mexico. *Remote Sensing of Environment*, 113(7), 1473-1485.
- Nagler, P. L., Glenn, E. P., Hursh, K., Curtis, C., & Huete, A. (2005). Vegetation mapping for change detection on an arid-zone river. *Environmental Monitoring and Assessment*, 109(1-3), 255-274.
- Newham, M. J., Fellows, C. S., & Sheldon, F. (2011). Functions of riparian forest in urban catchments: a case study from sub-tropical Brisbane, Australia. *Urban Ecosystems*, 14(2), 165-180.
- Ozesmi, S. L., & Bauer, M. E. (2002). Satellite remote sensing of wetlands. *Wetlands Ecology and Management*, 10, 381-402.
- Petersen, S. L., Stringham, T. K., & Laliberte, A. S. (2005). Classification of willow species using large-scale aerial photography. *Rangeland Ecology & Management*, 58(6), 582-587.

- Pettorelli, N., Vik, J. O., Mysterud, A., Gaillard, J. M., Tucker, C. J., & Stenseth, N. C. (2005). Using the satellite-derived NDVI to assess ecological responses to environmental change. *Trends in Ecology & Evolution*, 20(9), 503-510.
- Pilon-Smits, E. (2005). Phytoremediation. *Annual review of plant biology*, 56(1), 15-39.
- Proisy, C., Coueron, P., & Fromard, F. (2007). Predicting and mapping mangrove biomass from canopy grain analysis using Fourier-based textural ordination of IKONOS images. *Remote Sensing of Environment*, 109(3), 379-392.
- Pugh, R. E., Dick, D. G., & Fredeen, A. L. (2002). Heavy metal (Pb, Zn, Cd, Fe, and Cu) contents of plant foliage near the anvil range lead/zinc mine, Faro, Yukon Territory. *Ecotoxicology and Environmental Safety*, 52(3), 273-279.
- Rango, A., Laliberte, A., Herrick, J. E., Winters, C., Havstad, K., Steele, C., et al. (2009). Unmanned aerial vehicle-based remote sensing for rangeland assessment, monitoring, and management. *Journal of Applied Remote Sensing*, 3, 1-15.
- Rendong, L., & Jiyuan, L. Estimating wetland vegetation biomass in the Poyang Lake of central China from Landsat ETM data In *Geoscience and Remote Sensing Symposium - IGARSS '04 Proceedings.*, 2004 (Vol. 7, pp. 4590 - 4593): IEEE Conference Publications
- Richardson, D. M., Holmes, P. M., Esler, K. J., Galatowitsch, S. M., Stromberg, J. C., Kirkman, S. P., et al. (2007). Riparian vegetation: degradation, alien plant invasions, and restoration prospects. *Diversity and Distributions*, 13(1), 126-139.
- Runnells, D.D., Shepherd, T.A. & Angino, E.E. (1992): Metals in water – determining natural background concentrations in mineralized areas. *Environmental Science & Technology*, 26, 2316-2323.
- Salemi, L. F., Groppo, J. D., Trevisan, R., de Moraes, J. M., Lima, W. D., & Martinelli, L. A. (2012). Riparian vegetation and water yield: A synthesis. *Journal of Hydrology*, 454, 195-202.
- Samuelsson, F. (2010). Hornträsket - kvantifiering av bakgrundsläckage av metaller från mark till sjö. Masterthesis, Umeå University, Umeå.
- Schuft, M. J., Moser, T. J., Wigington, P. J., Stevens, D. L., & McAllister, L. S. (1999). Development of landscape metrics for characterizing riparian-stream networks. *Photogrammetric Engineering and Remote Sensing*, 65(10), 1157-1167.
- Sjöblom, Å. (2003). Wetlands as a means to reduce the environmental impact of mine drainage waters. Dotoral thesis, Linköping University, Linköping.
- Sjöblom, Å., Håkansson, K. & Allard, B. (2001): Metal concentrations along a mining region recipient – some aspects on water quality. In: *Proc. Securing Future – Int. Conf. Min. Environ.*, Skellefteå, Sweden, June 25-July 1, 2001, Vol. 2, pp. 777-786.
- Sjöblom, Å., Håkansson, K. & Allard, B. (2004): River water metal speciation in a mining region - the influence of wetlands, liming, tributaries, and groundwater. *Water, Air, and Soil Pollution* 152: 173-194.
- Sjörs, H. (1999). The background: Geology, climate and zonation. In H. Rydin, P. Snoeijs, & M. Diekmann (Eds.), *Swedish plant geography* (pp. 5-14). Uppsala: Svenska Växtgeografiska Sällskapet.
- Smith, T.M. and Smith R.L. (2006). *Elements of Ecology*. San Francisco: Pearson.
- StatSoft Inc. (2011). *Statistica 10*. Tulsa.
- Strayer, D. (2010). Ecology of freshwater shore zones. *Aquatic Sciences*, 72(2), 127-163.
- Swedish Environmental Protection Agency (Naturvårdsverket) (1999), *Bedömningsgrunder för miljö kvalitet - Sjöar och vattendrag*. Rapport 4913. Uppsala: Naturvårdsverket Förlag.

- Tabacchi, E., Correll, D. L., Hauer, R., Pinay, G., Planty-Tabacchi, A. M., & Wissmar, R. C. (1998). Development, maintenance and role of riparian vegetation in the river landscape. *Freshwater Biology*, 40(3), 497-516.
- Tabacchi, E., Lambs, L., Guillo, H., Planty Tabacchi, A. M., & Muller, E. (2000). Impacts of riparian vegetation on hydrological processes. *Hydrological Processes*, 14(16-17), 2959-2976.
- Tan, Q., Shao, Y., Yang, S., & Wei, Q. Wetland vegetation biomass estimation using Landsat-7 ETM+ data In *Geoscience and Remote Sensing Symposium - IGARSS '03 Proceedings, Toulouse, 21-25 July 2003 (Vol. 4, pp. 2629 - 2631): IEEE Conference Publications*
- Tempfli, K., Kerle, N., Huurneman, G. C., & Janssen, L. L. E. (Eds.). (2009). *Principles of Remote Sensing*. Enschede: ITC.
- Tormos, T., Kosuth, P., Durrieu, S., Villeneuve, B., & Wasson, J. G. (2011). Improving the quantification of land cover pressure on stream ecological status at the riparian scale using High Spatial Resolution Imagery. *Physics and Chemistry of the Earth*, 36(12), 549-559.
- Vandecasteele, B., De Vos, B., & Tack, F. M. G. (2002). Cadmium and Zinc uptake by volunteer willow species and elder rooting in polluted dredged sediment disposal sites. *Science of the Total Environment*, 299(1-3), 191-205.
- Wetzel, R. (2001). *Limnology*. San Diego, CA: Elsevier.
- Xiang, W., & Rengel, Z. (2009). Phytoremediation facilitates removal of nitrogen and phosphorus from eutrophicated water and release from sediment. *Environmental Monitoring and Assessment*, 157(1-4), 277-285.

8 APPENDIX I

Identified vegetation classes listed in order of decreasing total area (TA) for each locality. The area covered in the core zone (CZ) and extension zone (EZ) is also given. Rarely occurring species showed low frequency and low cover (CI).

ID-No.	Vegetation class	Rarely occurring species	TA [m ²]	CZ [m ²]	EZ [m ²]
L1 – riparian vegetation					
L1_1	<i>Betula pubescens</i> , <i>Calamagrostis canescens</i> , <i>Carex nigra</i> , <i>Carex nigra</i> ssp. <i>juncella</i> , <i>Carex rostrata/vesicaria</i> , <i>Molinia caerulea</i> , <i>Salix</i> sp.		2068		2068
L1_2	<i>Alnus incana</i> ssp. <i>incana</i> , <i>Betula nana</i> , <i>B. pubescens</i> , <i>C. canescens</i> , <i>C. nigra</i> ssp. <i>juncella</i> , <i>C. rostrata/vesicaria</i>		1240		1240
L1_3	<i>B. pubescens</i> , <i>C. canescens</i> , <i>Calamagrostis purpurea</i> , <i>C. nigra</i> ssp. <i>juncella</i> , <i>Salix</i> sp.	<i>C. rostrata/vesicaria</i> , <i>Carex</i> sp., <i>E. fluviatile</i> , <i>P. sylvestris</i>	1166	216	950
L1_4	<i>B. nana</i> , <i>C. canescens</i> , <i>C. rostrata/vesicaria</i> , <i>Eriophorum angustifolium</i> , <i>Salix</i> sp.	<i>B. pubescens</i> , <i>Calamagrostis</i> sp., <i>C. chordorrhiza</i> , <i>C. lasiocarpa</i> , <i>C. nigra</i> ssp. <i>juncella</i> , <i>Moneses uniflora</i> , <i>Picea abies</i> , <i>P. sylvestris</i> , <i>V. oxycoccus/microcarpum</i> , <i>V. uliginosum</i>	928	928	
L1_5	<i>Carex lasiocarpa</i> , <i>C. rostrata/vesicaria</i> , <i>E. angustifolium</i>		821		821
L1_6	<i>C. rostrata/vesicaria</i> , <i>E. angustifolium</i> , <i>Salix</i> sp.		696		696
L1_7	<i>B. pubescens</i> , <i>C. nigra</i> , <i>C. rostrata/vesicaria</i> , <i>M. caerulea</i> , <i>Salix</i> sp.		548		548
L1_8	<i>B. nana</i> , <i>C. lasiocarpa</i> , <i>C. rostrata/vesicaria</i> , <i>Salix</i> sp., <i>Trichophorum cespitosum</i>		531		531
L1_9	<i>B. pubescens</i> , <i>C. canescens</i> , <i>C. nigra</i> ssp. <i>juncella</i> , <i>C. rostrata/vesicaria</i> , <i>M. caerulea</i> , <i>Salix</i> sp.		427		427
L1_10	<i>B. pubescens</i> , <i>C. nigra</i> , <i>C. rostrata/vesicaria</i> , <i>E. angustifolium</i> , <i>Salix</i> sp.		388		388
L1_11	<i>C. nigra</i> , <i>C. rostrata/vesicaria</i> , <i>M. caerulea</i> , <i>Salix</i> sp.		383		383
L1_12	<i>B. nana</i> , <i>C. nigra</i> , <i>C. rostrata/vesicaria</i> , <i>Comarum palustre</i> , <i>Salix</i> sp.		361		361
L1_13	<i>C. canescens</i> , <i>C. purpurea</i> , <i>C. rostrata/vesicaria</i> , <i>E. angustifolium</i>		350		350

ID-No.	Vegetation class	Rarely occurring species	TA [m ²]	CZ [m ²]	EZ [m ²]
L1_14	<i>B. nana</i> , <i>B. pubescens</i> , <i>C. nigra</i> , <i>C. rostrata/vesicaria</i> , <i>Salix</i> sp.		332		332
L1_15	<i>B. pubescens</i> , <i>C. canescens</i> , <i>C. purpurea</i> , <i>C. nigra</i> ssp. <i>juncella</i> , <i>Equisetum fluviatile</i> , <i>Salix</i> sp.	<i>C. palustre</i> , <i>P. abies</i> , <i>P. sylvestris</i> , <i>Poaceae</i>	315	315	
L1_16	<i>C. nigra</i> , <i>C. rostrata/vesicaria</i> , <i>C. lasiocarpa</i> , <i>E. angustifolium</i>		259		259
L1_17	<i>Andromeda polifolia</i> , <i>B. nana</i> , <i>Carex chordorrhiza</i> , <i>Carex cespitosa</i> , <i>C. lasiocarpa</i> , <i>E. angustifolium</i> , <i>Salix</i> sp., <i>Vaccinium uliginosum</i>	<i>C. canescens</i> , <i>C. nigra</i> , <i>C. nigra</i> ssp. <i>juncella</i> , <i>C. rostrata/vesicaria</i> , <i>M. caerulea</i> , <i>P. sylvestris</i> , <i>Vaccinium microcarpum</i> , <i>V. oxycoccus</i>	255	255	
L1_18	<i>Salix</i> sp.	<i>B. nana</i> , <i>B. pubescens</i> , <i>Calamagrostis</i> sp., <i>C. canescens</i> , <i>C. rostrata/vesicaria</i> , <i>Carex</i> sp., <i>Poaceae</i>	247	88	159
L1_19	<i>B. nana</i> , <i>B. pubescens</i> , <i>C. nigra</i> , <i>C. nigra</i> ssp. <i>juncella</i> , <i>C. rostrata/vesicaria</i> , <i>Salix</i> sp.		246		246
L1_20	<i>B. nana</i> , <i>C. nigra</i> , <i>C. lasiocarpa</i> , <i>Equisetum arvense</i> ssp. <i>arvense</i> , <i>E. angustifolium</i> , <i>Salix</i> sp., <i>V. uliginosum</i>		243		243
L1_21	<i>B. pubescens</i> , <i>C. nigra</i> ssp. <i>juncella</i> , <i>C. lasiocarpa</i> , <i>M. caerulea</i> , <i>Salix</i> sp.		239		239
L1_22	<i>C. nigra</i> ssp. <i>juncella</i> , <i>M. caerulea</i> , <i>Salix</i> sp.		211		211
L1_23	<i>C. canescens</i> , <i>C. purpurea</i> , <i>E. angustifolium</i> , <i>Salix</i> sp.	<i>B. pubescens</i> , <i>C. lasiocarpa</i> , <i>C. nigra</i> ssp. <i>juncella</i> , <i>C. palustre</i> , <i>Poaceae</i>	201	87	114
L1_24	<i>C. rostrata/vesicaria</i>		180		180
L1_25	<i>B. nana</i> , <i>C. canescens</i> , <i>C. nigra</i> , <i>C. rostrata/vesicaria</i> , <i>Salix</i> sp.	<i>Agrostis</i> sp., <i>B. pubescens</i> , <i>C. chordorrhiza</i> , <i>C. cespitosa</i> , <i>C. lasiocarpa</i> , <i>E. angustifolium</i> , <i>P. sylvestris</i>	91	91	
L1_26	<i>C. nigra</i> ssp. <i>juncella</i> , <i>C. canescens</i> , <i>C. purpurea</i>	<i>B. pubescens</i> , <i>C. nigra</i> ssp. <i>juncella</i> , <i>E. fluviatile</i> , <i>P. sylvestris</i> , <i>Salix</i> sp.	88	49	38
L1_27	<i>C. nigra</i> ssp. <i>juncella</i>	<i>B. pubescens</i> , <i>C. nigra</i> ssp. <i>Juncella</i> , <i>C. rostrata/vesicaria</i> , <i>E. fluviatile</i> , <i>E. angustifolium</i> , <i>M. caerulea</i> , <i>Salix</i> sp.	66	34	32
L1_28	<i>C. canescens</i> , <i>C. rostrata/vesicaria</i>	<i>B. pubescens</i> , <i>E. fluviatile</i> , <i>Poaceae</i> , <i>Salix</i> sp.	56	56	
L1_29	<i>B. pubescens</i> , <i>C. rostrata/vesicaria</i> , <i>E. fluviatile</i> , <i>M. caerulea</i> , <i>Salix</i> sp.	<i>B. pubescens</i> , <i>C. purpurea</i> , <i>C. nigra</i> , <i>E. fluviatile</i> , <i>Poaceae</i>	46	46	

ID-No.	Vegetation class	Rarely occurring species	TA [m ²]	CZ [m ²]	EZ [m ²]
L1_30	<i>C. nigra</i> ssp. <i>juncella</i> , <i>C. rostrata/vesicaria</i> , <i>E. angustifolium</i>		15		15
L1_31	<i>B. pubescens</i> , <i>C. canescens</i> , <i>E. angustifolium</i> , <i>Salix</i> sp.	<i>C. purpurea</i> , <i>C. rostrata/vesicaria</i> , <i>Deschampsia cespitosa</i> , <i>E. angustifolium</i> , <i>M. caerulea</i> , <i>P. sylvestris</i> , <i>Pyrola media</i>	12	12	
L2 – riparian vegetation					
L2_1	<i>C. rostrata/vesicaria</i> , <i>E. angustifolium</i>	<i>C. nigra</i> , <i>Carex</i> sp., <i>P. abies</i> , <i>Poaceae</i> , <i>Salix</i> sp.	12020	7821	4199
L2_2	<i>C. rostrata/vesicaria</i> , <i>E. angustifolium</i> , <i>Salix</i> sp.		5439		5439
L2_3	<i>C. rostrata/vesicaria</i>	<i>E. fluviatile</i>	4785	1762	3023
L2_4	<i>C. lasiocarpa</i> , <i>C. rostrata/vesicaria</i> , <i>E. angustifolium</i>		4772		4772
L2_5	<i>B. pubescens</i> , <i>C. purpurea</i> , <i>C. nigra</i> ssp. <i>juncella</i> , <i>E. arvense</i> ssp. <i>arvense</i> , <i>Salix</i> sp.		779		779
L2_6	<i>A. polifolia</i> , <i>Calluna vulgaris</i> , <i>Trichophorum alpinum</i> , <i>T. cespitosum</i> , <i>V. uliginosum</i>		563		563
L2_7	<i>C. lasiocarpa</i> , <i>C. rostrata/vesicaria</i> , <i>E. angustifolium</i> , <i>Salix</i> sp.		516		516
L2_8	<i>C. nigra</i> , <i>C. rostrata/vesicaria</i> , <i>E. angustifolium</i> , <i>Salix</i> sp.		226		226
L2_9	<i>B. nana</i> , <i>C. rostrata/vesicaria</i> , <i>E. angustifolium</i> , <i>Salix</i> sp.		94		94
L2_10	<i>Salix</i> sp.		65		65
L2_11	<i>E. angustifolium</i>		59		59
L2_12	<i>B. nana</i> , <i>C. nigra</i> , <i>E. angustifolium</i> , <i>V. uliginosum</i>		57		57
L2 – vegetation from the river channel					
L2_13	<i>E. fluviatile</i>		4006		
L2_14	<i>Sparganium angustifolium</i>		763		
L2_15	<i>S. angustifolium</i> , <i>Hippuris vulgaris</i>		739		
L2_16	<i>Phragmites australis</i>		544		
L2_17	<i>Nuphar lutea</i>		458		
L2_18	<i>C. rostrata/vesicaria</i> , <i>P. australis</i>		297		
L2_19	<i>C. rostrata/vesicaria</i> , <i>E. fluviatile</i>		264		
L2_20	<i>E. fluviatile</i> , <i>H. vulgaris</i>		173		
L2_21	<i>E. fluviatile</i> , <i>S. angustifolium</i>		166		

ID-No.	Vegetation class	Rarely occurring species	TA [m ²]	CZ [m ²]	EZ [m ²]
L2_22	<i>H. vulgaris</i> , <i>Potamogeton alpinus</i> , <i>S. augustifolium</i>		80		
L2_23	<i>E. fluviatile</i> , <i>P. alpinus</i> , <i>S. augustifolium</i>		77		
L2_24	<i>E. fluviatile</i> , <i>N. lutea</i>		23		
L2_25	<i>S. augustifolium</i> , <i>Utricularia intermedia</i>		18		
L2_26	<i>N. lutea</i> , <i>S. augustifolium</i>		3		
L3 – riparian vegetation					
L3_1	<i>A. polifolia</i> , <i>B. pubescens</i> , <i>E. angustifolium</i> , <i>M. caerulea</i> , <i>Pinus sylvestris</i> , <i>T. cespitosum</i>	<i>C. nigra</i> ssp. <i>juncella</i> , <i>Carex panicea</i> , <i>C. palustre</i> , <i>J. filiformis</i> , <i>P. australis</i> , <i>Rubus articus</i> , <i>V. microcarpum</i> , <i>V. oxycoccus</i> , <i>V. uliginosum</i>	6358	529	5829
L3_2	<i>B. pubescens</i> , <i>C. nigra</i> , <i>C. nigra</i> ssp. <i>juncella</i> , <i>E. angustifolium</i> , <i>M. caerulea</i> , <i>Salix</i> sp.	<i>C. rostrata/vesicaria</i> , <i>Carex</i> sp., <i>C. palustre</i> , <i>Galium palustre</i> ssp. <i>palustre</i> , <i>Myosotis laxa</i> ssp. <i>caespitosa</i> , <i>P. australis</i> , <i>Trientalis europaea</i> , <i>V. oxycoccus</i> , <i>V. uliginosum</i> , <i>Viola epipsila/palustris</i>	3791	949	2842
L3_3	<i>B. pubescens</i> , <i>C. canescens</i> , <i>C. nigra</i> ssp. <i>juncella</i> , <i>M. caerulea</i> , <i>Pinus sylvestris</i> , <i>Salix</i> sp.		1908		1908
L3_4	<i>B. nana</i> , <i>B. Pubescens</i> , <i>C. vulgaris</i> , <i>Juncus filiformis</i> , <i>P. sylvestris</i> , <i>T. alpinum</i> , <i>T. Cespitosum</i> , <i>V. uliginosum</i>		1003		1003
L3_5	<i>C. nigra</i> , <i>C. lasiocarpa</i> , <i>C. rostrata/vesicaria</i> , <i>E. angustifolium</i>		866		866
L3_6	<i>C. nigra</i> , <i>C. nigra</i> ssp. <i>juncella</i> , <i>C. rostrata/vesicaria</i> , <i>E. angustifolium</i> , <i>Salix</i> sp.	<i>C. canescens</i> , <i>C. palustre</i> , <i>E. fluviatile</i> , <i>Peucedanum palustre</i> , <i>P. australis</i> , <i>P. sylvestris</i> , <i>U. intermedia</i>	608	212	396
L3_7	<i>C. lasiocarpa</i> , <i>C. nigra</i> , <i>E. angustifolium</i> , <i>M. caerulea</i> , <i>P. australis</i>		580		580
L3_8	<i>C. rostrata/vesicaria</i> , <i>E. angustifolium</i> , <i>P. australis</i>	<i>C. canescens</i> , <i>C. nigra</i> ssp. <i>juncella</i> , <i>C. palustre</i> , <i>G. palustre</i> ssp. <i>palustre</i> , <i>M. caerulea</i>	554	305	248
L3_9	<i>C. rostrata/vesicaria</i>		539		539
L3_10	<i>C. nigra</i> ssp. <i>juncella</i> , <i>E. angustifolium</i> , <i>M. caerulea</i> , <i>Salix</i> sp.		453		453
L3_11	<i>C. lasiocarpa</i> , <i>C. nigra</i> , <i>C. rostrata/vesicaria</i> , <i>E. angustifolium</i> , <i>P. australis</i> , <i>Salix</i> sp.		287		287
L3_12	<i>B. pubescens</i> , <i>C. purpurea</i> , <i>C. nigra</i> , <i>E. arvense</i> ssp. <i>arvense</i> , <i>M. caerulea</i> , <i>Salix</i> sp., <i>V. Uliginosum</i>		265		265
L3_13	<i>A. polifolia</i> , <i>B. nana</i> , <i>B. pubescens</i> , <i>J. filiformis</i> , <i>P. australis</i> , <i>P.</i>		233		233

ID-No.	Vegetation class	Rarely occurring species	TA [m ²]	CZ [m ²]	EZ [m ²]
	<i>sylvestris</i> , <i>T. cespitosum</i> , <i>V. uliginosum</i>				
L3_14	<i>C. nigra</i> ssp. <i>juncella</i> , <i>C. rostrata/vesicaria</i> , <i>M. caerulea</i>	<i>C. palustre</i> , <i>E. angustifolium</i> , <i>P. australis</i> , <i>Poaceae</i> , <i>Salix</i> sp., <i>T. europaea</i>	168	32	136
L3_15	<i>C. rostrata/vesicaria</i> , <i>E. angustifolium</i>		129		129
L3_16	<i>C. nigra</i> , <i>C. rostrata/vesicaria</i> , <i>E. angustifolium</i> , <i>Salix</i> sp.		109		109
L3_17	<i>C. nigra</i> , <i>C. rostrata/vesicaria</i> , <i>E. angustifolium</i> , <i>M. caerulea</i>	<i>A. polifolia</i> , <i>C. lasiocarpa</i> , <i>C. nigra</i> ssp. <i>juncella</i> , <i>Carex</i> sp., <i>C. palustre</i> , <i>P. sylvestris</i> , <i>Salix</i> sp.	106	34	72
L3_18	<i>B. pubescens</i> , <i>C. nigra</i> , <i>E. angustifolium</i> , <i>M. caerulea</i> , <i>Pinus</i> <i>sylvestris</i> , <i>T. cespitosum</i>		100		100
L3_19	<i>B. pubescens</i> , <i>C. canescens</i> , <i>C. nigra</i> ssp. <i>juncella</i> , <i>C.</i> <i>rostrata/vesicaria</i> , <i>Salix</i> sp.	<i>C. palustre</i> , <i>E. angustifolium</i> , <i>G. palustre</i> ssp. <i>palustre</i> , <i>M. caerulea</i> , <i>P. palustre</i> , <i>P. australis</i> , <i>P.</i> <i>sylvestris</i>	67	67	
L3_20	<i>C. lasiocarpa</i> , <i>E. angustifolium</i> , <i>M. caerulea</i> , <i>T. cespitosum</i>		43		43
L3_21	<i>A. polifolia</i> , <i>C. nigra</i> , <i>E. angustifolium</i> , <i>M. caerulea</i> , <i>Vaccinium</i> <i>oxycoccus</i>	<i>B. pubescens</i> , <i>C. nigra</i> ssp. <i>juncella</i> , <i>T. cespitosum</i>	41	41	
L3_22	<i>C. lasiocarpa</i> , <i>C. nigra</i> , <i>E. angustifolium</i> , <i>M. caerulea</i> , <i>Salix</i> sp.	<i>B. pubescens</i> , <i>C. rostrata/vesicaria</i> , <i>V. oxycoccus</i> , <i>V.</i> <i>epipsila/palustris</i>	31	31	
L3_23	<i>B. pubescens</i> , <i>Carex buxbaumii</i> ssp. <i>buxbaumii</i> , <i>C. flava</i> , <i>C.</i> <i>nigra</i> , <i>C. rostrata/vesicaria</i> , <i>Salix</i> sp., <i>V. uliginosum</i>		28		28
L3_24	<i>A. polifolia</i> , <i>C. nigra</i> , <i>E. angustifolium</i> , <i>M. caerulea</i>	<i>A. polifolia</i> , <i>B. nana</i> , <i>C. nigra</i> ssp. <i>juncella</i> , <i>C.</i> <i>palustre</i> , <i>Salix</i> sp., <i>V. microcarpum</i>	24	24	
L3_25	<i>C. rostrata/vesicaria</i> , <i>E. angustifolium</i> , <i>Salix</i> sp.		23		23
L3_26	<i>Carex canescens</i> , <i>C. rostrata/vesicaria</i> , <i>J. filiformis</i> , <i>P. australis</i>		12		12
L3_27	<i>Salix</i> sp.		1		1
L3 – vegetation from the river channel					
L3_28	<i>N. lutea</i> , <i>Nymphaea alba</i> ssp. <i>candida</i>		1541		
L3_29	<i>C. rostrata/vesicaria</i> , <i>P. australis</i>		279		
L3_30	<i>Potamogeton gramineus</i>		258		
L3_31	<i>N. lutea</i> , <i>N. alba</i> ssp. <i>candida</i> , <i>P. gramineus</i>		208		
L3_32	<i>P. australis</i> , <i>P. gramineus</i>		73		

ID-No.	Vegetation class	Rarely occurring species	TA [m ²]	CZ [m ²]	EZ [m ²]
L3_33	<i>N. lutea</i> , <i>N. alba</i> ssp. <i>candida</i> , <i>Sparganium</i> sp.			28	
L3_34	<i>H. vulgaris</i> , <i>N. lutea</i> , <i>N. alba</i> ssp. <i>candida</i> , <i>P. gramineus</i>			14	
L3_35	<i>H. vulgaris</i> , <i>P. gramineus</i>			10	